Advanced Drug Delivery Reviews 109 (2017) 84–101

Contents lists available at ScienceDirect

Advanced Drug Delivery Reviews

journal homepage: www.elsevier.com/locate/addr

Gold nanoparticles for applications in cancer radiotherapy: Mechanisms and recent advancements☆

Sohyoung Her [a], David A. Jaffray [b,c,d,e,f,g], Christine Allen [a,e,g,*]

[a] Department of Pharmaceutical Sciences, Leslie Dan Faculty of Pharmacy, University of Toronto, Toronto, Ontario M5S 3M2, Canada
[b] Department of Radiation Oncology, University of Toronto, Toronto, Ontario, Canada
[c] Department of Medical Biophysics, University of Toronto, Toronto, Ontario, Canada
[d] Department of Radiation Physics, Princess Margaret Cancer Centre, University Health Network, Toronto, Ontario, Canada
[e] STTARR Innovation Centre, Radiation Medicine Program, Princess Margaret Cancer Centre, University Health Network, Toronto, Ontario, Canada
[f] Techna Institute, University Health Network, Toronto, Ontario, Canada
[g] Institute of Biomaterials and Biomedical Engineering, University of Toronto, Toronto, Ontario, Canada

ARTICLE INFO

Article history:
Received 24 October 2015
Received in revised form 10 December 2015
Accepted 11 December 2015
Available online 19 December 2015

Keywords:
Radiosensitization
Radiation therapy
Gold nanoparticle
Mechanism
Multi-functional nanoplatform
Hypoxic radiosensitizer
Active targeting
Ion radiotherapy

ABSTRACT

Gold nanoparticles (AuNPs) have emerged as novel radiosensitizers owing to their high X-ray absorption, synthetic versatility, and unique chemical, electronic and optical properties. Multi-disciplinary research performed over the past decade has demonstrated the potential of AuNP-based radiosensitizers, and identified possible mechanisms underlying the observed radiation enhancement effects of AuNPs. Despite promising findings from pre-clinical studies, the benefits of AuNP radiosensitization have yet to successfully translate into clinical practice. In this review, we present an overview of the current state of AuNP-based radiosensitization in the context of the physical, chemical and biological modes of radiosensitization. As well, recent advancements that focus on formulation design and enable multi-modality treatment and clinical utilization are discussed, concluding with design considerations to guide the development of next generation AuNPs for clinical applications.

Contents

Abbreviations: 5′-ALA, 5′-aminolevulinic acid; Au, gold; AuNC, gold nanocapsule; AuNP, gold nanoparticle; AuNR, gold nanorod; BSA, bovine serum albumin; CT, computed tomography; DEF, dose enhancement factor; DNA, deoxyribonucleic acid; DOX, doxorubicin; DSB, double strand break; EB, external beam; EGFR, epidermal growth factor receptor; EPR, enhanced permeability retention effect; FA, folic acid; FDG, fluoro-deoxyglucose; Glu, glucose; GPM, gold-loaded polymeric micelles; GSH, glutathione; GSM, gold- and SPION-loaded polymeric micelles; HER2, human epidermal growth factor receptor 2; HGNPs, hollow gold nanoparticles; ID, injected dose; IR, ionizing radiation; kV, kilovoltage; LEE, low energy electron; LET, low energy transfer; LINAC, linear accelerator; LSPR, local surface plasmon resonance; MCTS, multi-cellular tumor spheroid; MR, magnetic resonance; MUA, mercaptoundecanoic acid; MV, megavoltage; NAC, *N*-acetyl cysteine; NIR, near-infrared; NLS, nuclear localization signal; PCL, poly(ε-caprolactone); PEG, poly(ethylene glycol); PET, positron emission tomography; PK, pharmacokinetic; PTT, photothermal therapy; RBE, relative biological effectiveness; RES, reticulo-endothelial system; rhTNF, recombinant human tumor necrosis factor alpha; RME, receptor-mediated endocytosis; RNA, ribonucleic acid; ROS, reactive oxygen species; RT, radiotherapy; SER, sensitizer enhancement ratio; SF, surviving fraction; SPION, superparamagnetic iron oxide nanoparticle; SSB, single strand break; TrxR1, thioredoxin reductase 1; Z, atomic number.

☆ This review is part of the *Advanced Drug Delivery Reviews* theme issue on "Radiotherapy for Cancer: Present and Future".

* Corresponding author at: Department of Pharmaceutical Sciences, Leslie Dan Faculty of Pharmacy, University of Toronto, 144 College Street, Toronto, Ontario M5S 3M2, Canada.
E-mail address: cj.allen@utoronto.ca (C. Allen).

http://dx.doi.org/10.1016/j.addr.2015.12.012
0169-409X/

1. Introduction

Radiotherapy (RT), alongside surgery and chemotherapy, is one of the most effective modes of cancer treatment, with over 50% of all patients receiving RT with curative or palliative intent [1,2]. In RT, ionizing radiation (IR) is delivered to the tumor via an external beam (EB) or from an internally placed radiation source (brachytherapy). Exposure to IR causes damage to various cellular components, with the DNA being the most critical target, directly or indirectly via ionization of molecules (e.g. water) within the cells, generating a cascade of free radicals. While effective at achieving tumor control, the surrounding normal tissues are also affected by the IR. As a result, the dose of radiation administered must be limited in order to keep normal tissue toxicities at a tolerable level. Considerable improvements have been made in RT over the past few decades, with a particular emphasis on the recent technological advances that enable precision in the delivery of radiation via intensity modulation in combination with image guidance [3–7]. As well, with an increasing understanding of the molecular pathways involved in radiation response, personalized treatment approaches that utilize molecularly targeted drugs are under investigation to achieve tumor-specific targeting of IR [8,9].

Nanotechnology, which offers a number of unique features suited for applications in oncology, has also emerged as a promising strategy to enhance radiotherapeutic efficacy. By exploiting the enhanced permeability and retention (EPR) effect, the preferential accumulation of nanoparticles in the tumor may lead to (1) improved contrast enhancement for image-guided RT, (2) tumor-specific delivery of chemotherapeutic agents for combined chemo-RT, and (3) an increased local dose of radiation using particles with high atomic numbers (Z). Among various nano-platforms investigated for radiotherapeutic applications, gold nanoparticles (AuNPs) have been most extensively studied due to their high X-ray absorption coefficient, as well as the ease of synthetic

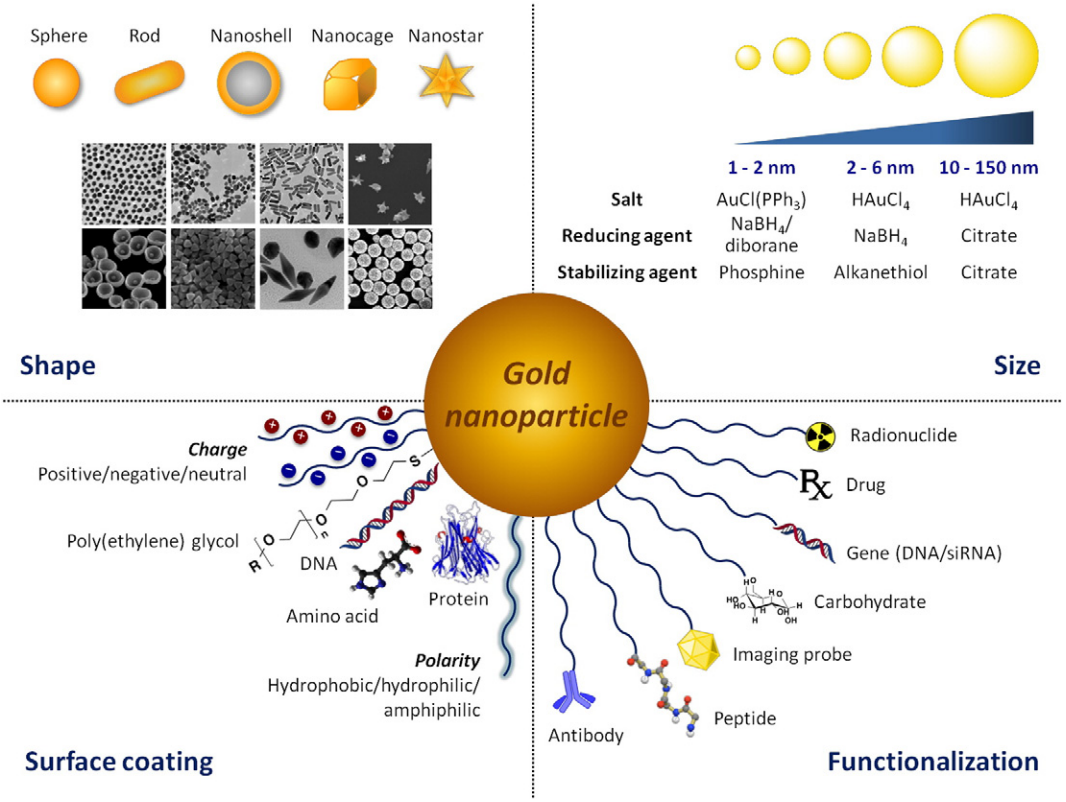

Fig. 1. The synthetic versatility of AuNPs. AuNPs offer a unique platform for straightforward manipulation of particle size, shape, surface coating and functionalization, enabling fine-tuning of particle properties. Adapted with permission from [10–15].

manipulation, enabling precise control over the particle's physico-chemical properties.

AuNPs are colloidal or clustered particles with diameters in the range of a few to several hundreds of nanometers that consist of a Au core and a surface coating. One of the advantageous features of AuNPs is the synthetic versatility, which enables fine tailoring of the particle size, shape and surface properties (Fig. 1). Size and shape control can be easily achieved to obtain AuNPs in the range of 1–150 nm with diverse morphologies that offer unique chemical, electrical and optical properties [16–22]. In addition to the Au core that defines the fundamental characteristics of a AuNP, a protective coating that surrounds the core can also be modified to control particle stability, solubility and interaction with the biological environment [23,24]. As well, the ability of the AuNP surface to bind thiols and amines provides a convenient way to introduce reactive functional groups that can be utilized for labeling (e.g. imaging probes), targeting (e.g. antibodies, peptides), and conjugating therapeutic agents (e.g. drugs, radionuclides). Taking advantage of the synthetic versatility combined with the unique optical and electronic properties of Au, AuNPs have been exploited for a wide variety of biomedical applications, including imaging (e.g. computed tomography, photoacoustic imaging, surface enhanced Raman scattering), delivery (e.g. drugs, genes, small-interfering RNAs) and therapy (e.g. photothermal therapy, radiosensitization) as well as inclusion in diagnostic platforms (e.g. biological and chemical sensing) (Fig. 2) [25–30].

Seminal work conducted by Hainfeld et al. in 2004 provided the first experimental evidence of the radiation dose enhancement effects of AuNPs *in vivo*, which ignited exponential growth in the field of AuNP radiosensitization [33]. In this study, treatment with 1.9 nm AuNPs in combination with 30 Gy irradiation (250 kVp X-rays) resulted in a drastic increase in the one-year survival of mice bearing subcutaneous EMT-6 mammary carcinoma from 20% with X-rays alone to 50% with 1.35 g Au/kg, and further to 86% with a higher dose of AuNPs (2.7 g Au/kg). Since this pioneering work, a large number of studies have demonstrated the ability of AuNPs to effectively sensitize cells to both kilovoltage (kV) and megavoltage (MV) radiation *in vitro* (Table 1) and *in vivo* (Table 2). As well, new modes of radiosensitization beyond the initially established physical enhancement effects have been identified, shining light on the factors that influence the radiosensitization potential of AuNPs.

Reflecting upon the promising findings of the research performed over the past decade, this review aims to provide a discussion of the current status and future directions in the field of AuNP-based radiosensitization. In Section 2, we present an overview of the mechanisms underlying the observed dose enhancement effects with AuNPs. In Section 3, recent advancements, particularly in the context of formulation design that exploit the synthetic versatility of the AuNP platform, as well as the clinically relevant applications of AuNP radiosensitizers, are highlighted. Finally in Section 4, the factors that influence radiosensitization and the corresponding design considerations for AuNPs are discussed with a goal towards developing the ideal AuNP-based radiosensitizer for successful clinical translation.

2. Mechanisms of AuNP radiosensitization

Upon exposure to IR, biological systems undergo a series of processes that can be divided into three phases, namely, physical, chemical and biological that differ in terms of time scale [1,62]. In the physical phase, which occurs within the first nanoseconds of exposure, IR interacts with biomolecules to cause ionization or excitation, generating free radicals. Among various cellular components, DNA is the major target that determines the radiobiological effects. Given sufficient energy, the ejected electrons travel further to collide with subsequent atoms to create a cascade of ionization events. In the chemical phase, these highly reactive

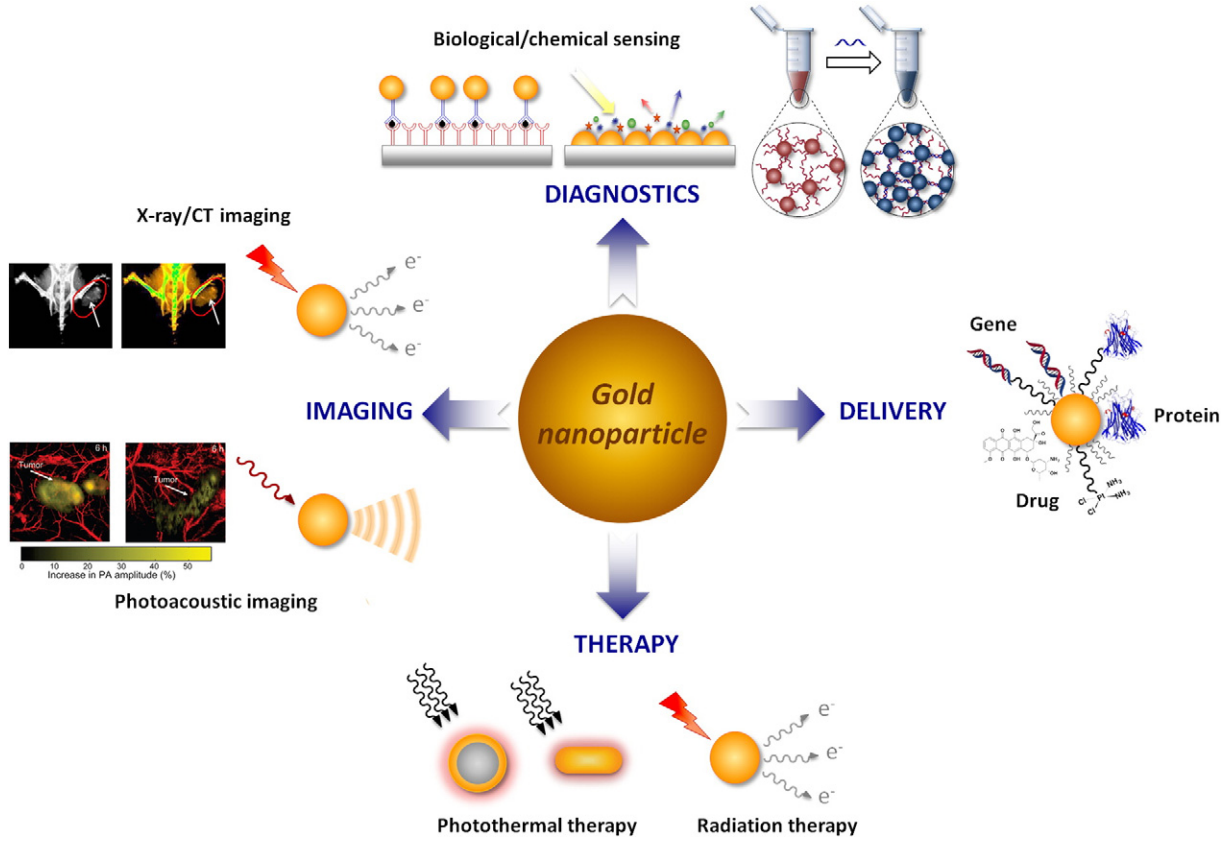

Fig. 2. Biomedical applications of AuNPs. Owing to their unique physico-chemical, optical and electronic properties, AuNPs have been exploited for a wide range of applications in diagnostics, imaging, delivery, and therapy. Adapted with permission from [31] and [32].

Table 1
Summary of *in vitro* studies on AuNP radiosensitization.

Author [Ref]	Size	Conc.	Surface	Cell line	Energy	DEF/Effect
Butterworth et al. [34]	1.9 nm	2.4 μM 0.24 μM	Proprietary thiol (AuroVist™)	AGO-1552B Astro DU-145 L132 MCF-7 MDA-MB-231 PC-3 T98G	160 kVp	1.97 0.96 0.81 0.87 1.09 1.11 1.02 1.91
Chang et al. [35]	13 nm	10 nM	Citrate	B16F10	6 MeV e^-	Significant decrease in SF at 8 Gy with AuNPs vs. IR alone
Chattopadhyay et al. [36]	30 nm	2.4 mg/mL	PEG HER2 targeted (trastuzumab)	MDA-MB-361	100 kVp	1.6 (targeted) 1.3 (non-targeted)
Chen et al. [37]	28 nm (18 nm core)	36 μg/mL	BSA	U87	160 kVp	1.37
Chithrani et al. [38]	14 nm 50 nm 74 nm	7 x 10^9 NPs/mL	Citrate-AuNPs	HeLa	105 kVp 220 kVp 660 keV (137-Cs) 6 MVp	1.66 1.43 1.18 1.17
Coulter et al. [39]	1.9 nm	12 μM (500 μg/mL)	Proprietary thiol (AuroVist™)	MDA-MB-231 DU145 L132	160 kVp	~1.8 (MDA-MB-231)
Cui et al. [40]	2.7 nm	0.5 mg/mL	Tiopronin	MDA-MB-231	225 kVp	1.04–1.44
Geng et al. [41]	14 nm	1.25, 2.5, 5 nM	Glucose	SK-OV-3	90 kVp 6 MV	1.44 1.3–1.37
Jain et al. [42]	1.9 nm	12 μM (500 μg/mL)	Proprietary thiol (AuroVist™)	MDA-MB-231	160 kVp	1.41
Jain et al. [43]	1.9 nm	12 μM (500 μg/mL)	Proprietary thiol (AuroVist™)	MDA-MB-231 L132 DU145	160 kVp 6 MV 15 MV	1.41 1.29 1.16 (MDA-MB-231)
Joh et al. [44]	12 nm	1 mM	PEG	U251	150 kVp	~1.3
Kaur et al. [45]	5–9 nm	5.5 μmol/mL	Glucose	HeLa	Gamma (60-Co) Carbon (62 MeV)	1.52 1.39
Khoshgard et al. [46]	47–52 nm	50 μM	PEG, Folate-conjugated	HeLa	Gamma (60-Co)	1.64 (targeted) 1.35 (untargeted)
Kong et al. [47]	10.8 nm	15 μM	Cysteamine or glucose	MCF-7	200 kVp 662 keV (137-Cs) 60-Co	~1.3 (cysteamine) ~1.6 (glucose)
Liu et al. [48]	6.1 nm	0.4–1 mM	PEG	EMT-6 CT26	6.5 keV 8.048 keV 160 kVp 6 MeV 3 MeV proton	~2–45% decrease in survival rate
Liu et al. [49]	4.7 nm	500 μM	PEG	CT26	6 MV	1.33–1.59
Liu et al. [50]	14.8 nm	1.5–15 μg/mL	Citrate	HeLa	50 kVp X-rays 70 keV/μm carbon	1.14–2.88 1.27–1.44
Rahman et al. [51]	1.9 nm	0.25, 0.5, 1 mM	Proprietary thiol (AuroVist™)	BAEC	80 kVp 150 kVp 6 MeV 12 MeV	20 1.4 2.9 3.7 (at 0.5 mM)
Roa et al. [52]	10.8 nm	15 nM	Glucose	DU-145	662 keV (137-Cs)	1.24–1.38
Taggart et al. [53]	1.9 nm	12 μM (500 μg/mL)	Proprietary thiol (AuroVist™)	MDA-MB-231 T98G DU-145	225 kVp	1.17–1.23 (MDA-MB-231) 1.35–1.90 (T98G) 1.01–1.1 (DU-145)
Wang et al. [54]	13 nm	20 nM	Glucose	A549	6 MV	1.49
Wang et al. [55]	16 nm, 49 nm	20 nM	Glucose	MDA-MB-231	6 MV	1.49 (16 nm) 1.86 (49 nm)
Wolfe et al. [56]	31 × 9 nm	0.3 optical density	PEG, goserelin-conjugated nanorods	PC3	6 MV	1.19 (non-targeted) 1.36 (targeted)
Zhang et al. [57]	30 nm	15 nM	Glucose	DU-145	200 kVp	>1.3
Zhang et al. [58]	4.8, 12.1, 27.3, 46.6 nm	0.05 mM	PEG	HeLa	662 keV (137-Cs)	20 nM 1.41 (4.8 nm) 1.65 (12.1 nm) 1.58 (27.3 nm) 1.42 (46.6 nm)
Zhang et al. [59]	<2 nm	50 μg/mL	Glutathione (GSH) or BSA	HeLa	662 keV (137-Cs)	~1.3 (GSH) ~1.21 (BSA)

Table 2
Summary of *in vivo* studies on AuNP radiosensitization.

Author	Size	Surface	Injection dose (i.v./i.t./i.p.)	Cell model	Energy	Outcome
Chang et al. [35]	13 nm	Citrate	200 μL, 200 nM AuNPs i.v.	B16F10	6 MeV e^-	Significant tumor growth delay; increase in survival
Chattopadhyay et al. [36]	30 nm	PEG HER2 targeted (trastuzumab)	~0.8 mg Au (4.8 mg/g tumor) i.t.	MDA-MB-361	100 kVp, 11 Gy	Tumor growth inhibition (46% vs. 16%)
Chen et al. [37]	28 nm (18 nm core)	BSA	1.3 mg/mL (250 μL) i.v.	U87	160 kVp, 3 Gy at 2 h post-inj + 2 Gy at 24 h post-injection	Tumor regression
Hainfeld et al. [33]	1.9 nm	Proprietary thiol (AuroVist™)	1.35 g Au/kg 2.7 g Au/kg i.v.	EMT-6	250 kVp, 26 Gy	50% long-term survival (>1 year) at 1.35 g Au/kg 86% long-term survival (>1 year) at 2.7 g Au/kg
Hainfeld et al. [60]	1.9 nm	Proprietary thiol (AuroVist™)	1.9 g /kg i.v.	SCCVII	68 keV, 42 Gy 157 keV, 50.6 Gy	Increase in median survival (53 vs. 76 days at 68 keV; 31 vs. 49 days at 157 keV)
Hainfeld et al. [61]	1.9 nm	Proprietary thiol (AuroVist™)	4 g Au/kg i.v.	Tu-2449	100 kVp, 30 Gy	50% long-term tumor-free survival (>1 year)
Joh et al. [44]	12 nm	PEG	1.25 g Au/kg i.v.	U251	175 kVp, 20 Gy	Median survival (28 vs. 14 days)
Wolfe et al. [56]	31 × 9 nm	PEG, goserelin-conjugated nanorods	100 μL, 40 μM AuNPs i.v.	PC3	6 MV	Tumor growth delays 17 days (targeted) and 3 days (untargeted)
Zhang et al. [58]	4.8, 12.1, 27.3, 46.6 nm	PEG	4 mg/kg i.v.	HeLa	662 keV (137-Cs)	Tumor growth inhibition
Zhang et al. [59]	< 2 nm	Glutathione (GSH) or BSA	10 mg/kg i.p.	U14	662 keV (137-Cs)	~55 (GSH-AuNPs) and ~38% (BSA-AuNPs) decrease in tumor volume

radicals undergo rapid reactions to permanently fix the damage or engage in scavenging reactions to restore cellular charge equilibrium. In the final biological phase, a series of cellular processes are activated to repair the radiation-induced damage, and the failure to successfully repair ultimately leads to cell kill over a span of seconds to days, or even years.

Radiosensitization by AuNPs was initially believed to stem solely from physical dose enhancement, exploiting the elevated photoelectric absorption of Au. However, additional chemical and biological contributions to radiosensitization became evident with more experimental data, suggesting roles for AuNPs in all three phases of interactions with IR (Fig. 3). While the precise mechanisms underlying AuNP-induced dose enhancement remain to be fully elucidated, several modes of radiosensitization have been proposed. In the following subsections, these mechanisms are discussed in the context of the three different phases of radiation effects on biological systems.

2.1. Physical enhancement

The main rationale for developing AuNP radiosensitizers is based on differences in the energy absorbing properties of Au compared to soft tissues, enabling physical dose enhancement in the presence of Au. In

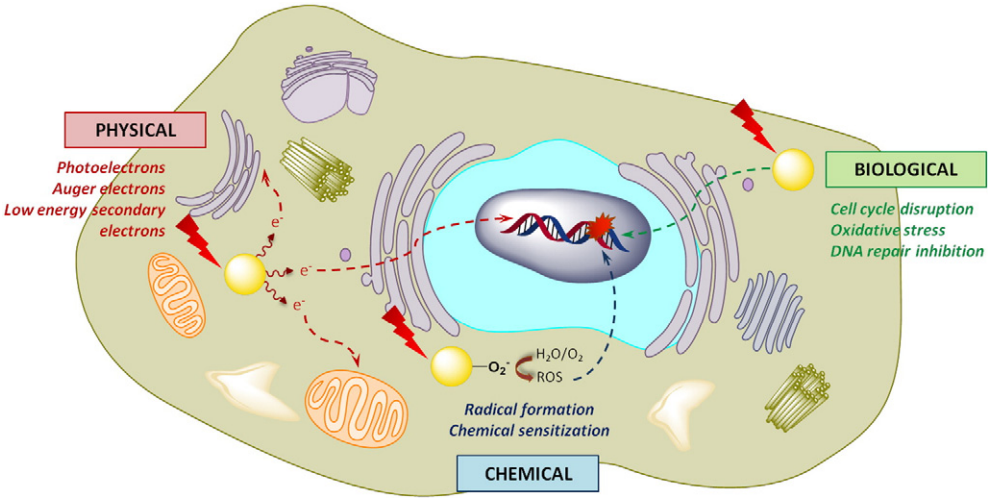

Fig. 3. Mechanisms of AuNP radiosensitization. AuNPs enhance radiation effects via physical, chemical and biological interactions with IR. In the physical phase of interactions, AuNPs exert cellular damage by increasing the production of photoelectrons, Auger electrons and low energy secondary electrons. In the chemical phase, the electronically active surface of AuNPs catalyzes the formation of radicals including ROS, and the very low energy electrons chemically sensitize the DNA to IR-induced damage. Finally, in the biological phase, AuNPs enhance the effects of IR via oxidative stress, cell cycle disruption, and DNA repair inhibition.

the kV energies, photons interact with matter mainly through the Compton effect or the photoelectric effect. In the Compton effect, an incident photon is scattered upon collision with a weakly bound electron. In this process, some of the energy is transferred from the photon to the electron, and the electron is ejected from the atom. In the photoelectric effect, an incident photon is absorbed by an atom-bound electron leading to the ejection of an inner-shell electron. As the outer-shell electrons fall to fill the vacancy, lower energy photons (fluorescence) and a cascade of secondary electrons (Auger electrons) are released. In contrast to the Compton effect, the photoelectric effect is strongly dependent on the photon energy as well as the binding energy of the electron. Consequently, the X-ray cross section, which refers to the probability of material interacting with radiation, is dependent on the atomic number (Z) of the interacting atom, scaling approximately as Z^4. By exploiting the atomic number difference between Au ($Z = 79$) and soft tissues, which are primarily composed of organic materials with low atomic numbers, AuNPs can be used to deliver a significantly greater amount of energy per unit mass, increasing the local dose of radiation deposited at the target site (i.e. tumor).

The first evidence of Z-material radiosensitization using Au was demonstrated by Regulla et al. using a thin layer of Au foil adsorbed on to the surface of a poly(methylmethacrylate) slab [63]. Irradiation of mouse embryo fibroblasts placed in contact with the Au surface resulted in radiation dose enhancements, achieving DEFs of up to 50. This finding was further supported by Herold et al. who reported dose enhancements (DEF = 1.43) in rodent or human cancer cell suspensions irradiated with 200 kVp X-rays in the presence of Au microspheres (1.5–3.0 μm) [64]. While lower energy photons successfully radiosensitized cells *in vitro*, irradiation with higher energy photons (137-Cs, 667 keV γ-rays) failed to produce dose enhancement. This differential radiosensitization effects were attributed to the diminished contribution of the photoelectric absorption by Au at higher energies, providing support for physical dose enhancement by Au.

Based on the early reports of Z-material radiosensitization by Au, combined with the rapid growth of interest in nanomedicine, AuNPs have been developed as novel agents for RT. The physical effects of AuNP radiosensitization have been demonstrated in studies with plasmid DNA, which enable the assessment of radiation-induced DNA damage at the molecular level in the absence of biological responses to radiation. These studies revealed that the energy released by AuNPs is nanoscale in nature, and that the low energy electrons (LEEs) play a critical role in dose enhancement by AuNPs. Carter et al. examined the distribution of electrons emitted from 3 nm AuNPs intercalated with DNA upon irradiation with 100 kVp X-rays, and showed that the DNA damage was caused mostly by LEEs (< 100 eV) that have effective ranges of 1–10 nm [65]. DNA damage by long range photoelectrons that can travel up to micrometers was negligible. Similar results were observed by Zheng et al. who reported a 2.5-fold increase in double strand breaks (DSBs) and single strand breaks (SSBs) when DNA-AuNP complexes were exposed to 60 keV radiation compared to the irradiation of pure DNA [66]. As well, experiments with DNA films of different thicknesses adsorbed onto gold foil showed significantly greater radiation-induced DNA damage to the thin (10 nm) film compared to the thick (2900 nm) film, highlighting the importance of short range electrons. Experimental findings from these plasmid DNA studies suggest that secondary LEEs generated from AuNPs result in localized energy deposition in the vicinity of the nanoparticle, leading to radiosensitization.

2.2. Chemical enhancement

In comparison to the physical and biological pathways of radiation enhancement by AuNPs, chemical enhancement has not been extensively investigated. Despite the limited number of studies, findings to date suggest a significant influence on the radiation effects even at low concentrations of Au, highlighting the importance of a chemical contribution to radiosensitization. The role of AuNPs in the chemical phase of radiation exposure is through involvement in radical reactions that fix the damage, or via weakening of DNA bonds, rendering DNA more susceptible to radiation-induced damage. Depending on the cellular localization of AuNPs, two possible mechanisms of chemical enhancement have been proposed: (1) chemical sensitization of DNA to IR-induced damage, and (2) increased radical formation and catalysis via the activated surface of AuNPs. While both processes could lead to increased radiosensitization, the first mechanism requires nuclear localization of AuNPs to permit binding to DNA. Unfortunately, the vast majority of AuNPs studied to date have shown endo/lysosomal entrapment of AuNPs in the cytosol, restricting nuclear entry. Nonetheless, both processes provide critical insight into the mechanism of AuNP radiosensitization, which in turn, guide the design of ideal nanoparticles to achieve maximum dose enhancement effects.

2.2.1. Chemical sensitization of DNA to radiation

In addition to the contribution by secondary electrons, very LEEs with energies below the ionization threshold (i.e. insufficient energy to ionize matter, <10 eV) have been shown to play a role in radiosensitization. Using electrons of different energies (1, 10, 100, 60,000 eV), Sanche's group demonstrated that 10 eV electrons, which do not produce considerable secondary electrons upon interactions with AuNPs, caused the greatest DNA damage [67]. This result was attributed to the very LEE-induced formation of transient negative ions that weaken the bonds within DNA, chemically sensitizing DNA to damage by LEEs emitted from AuNPs. In a recent publication, the same group prepared two types of AuNPs that differ in size and charge to further demonstrate the role of very LEEs in AuNP radiosensitization [68]. In this study, DNA-AuNP complexes were prepared with positively-charged 5 nm AuNPs or negatively-charged 15 nm AuNPs, and the DNA damage induced by 10 eV electrons was examined. It was found that the tight binding of the small, positive AuNPs to the PO_4 groups of DNA led to significant damage, achieving an enhancement factor of 4.5 at a 1:1 ratio of DNA:AuNPs. On the other hand, the large, negative AuNPs showed a much weaker and more random binding to DNA, resulting in a substantially lower degree of radiosensitization compared to the smaller AuNPs. Based on these findings, small AuNPs that are capable of nuclear localization and tight electrostatic binding to DNA were recommended to enable full exploitation of the chemical enhancement.

2.2.2. AuNP-catalyzed radical production

In contrast to the widely-accepted notion that AuNPs are chemically inert, an increasing number of studies have reported that the surface of AuNPs is electronically active and is capable of catalyzing chemical reactions [69–72]. In particular, small particles (<5 nm) with large surface area have been shown to exhibit superior catalytic activity via AuNP-mediated transfer of electrons from surface-bound donor groups to O_2 to generate superoxide radicals [73,74]. The unique catalytic properties of AuNPs were attributed to the small size and high curvature of the nanoparticles that disrupt the highly organized crystal structure of bulk Au. The alteration in the electronic configuration of surface atoms enables radical production at the reactive surface of AuNPs [74].

The catalytic activity of the AuNP surface has also been demonstrated in cellular systems. For instance, Ito et al. showed that 15 nm citrate-AuNPs potentiate the cytotoxic effects of 5′-aminolevulinic acid (5′-ALA), a precursor of heme that is commonly used in photodynamic therapy, by enhancing reactive oxygen species (ROS) production [75]. The combination of 5′-ALA and AuNPs catalyzes the formation of superoxide and hydroxyl radicals in a two-step process involving the interaction of 5′-ALA with the AuNP surface followed by binding of molecular oxygen to generate ROS. In addition to this study, a number of reports have demonstrated enhanced ROS production *in vitro* in the absence of radiation [39,74,76–80]. These studies confirmed that catalysis by AuNPs occurs predominantly through surface interaction with molecular oxygen, which facilitates surface-mediated transfer of electrons to generate ROS. In combination with IR, the catalytic properties of

AuNPs have shown to be further enhanced by interacting with the highly reactive environment formed by X-ray irradiation. Misawa et al. reported that the addition of AuNPs to water led to a 1.46- and 7.68-fold increase in hydroxyl radicals ($^{\bullet}OH$) and superoxide anions (O_2^-), respectively, upon irradiation with 100 kVp X-rays [81]. The enhancement in ROS production was attributed to the AuNP-induced emission of photo- and Auger-electrons, as well as fluorescent X-rays, which cause secondary radiolysis of water via charge-transfer. As well, evaluation of the relationship between particle size and ROS production revealed that smaller AuNPs with larger surface area yielded higher levels of ROS, further confirming the catalytic role of the AuNP surface. The enhanced catalytic activity of AuNPs was also observed by Cheng et al., in which superoxides generated by X-ray irradiation activated the surface atoms of AuNPs, chemically enhancing the effect of radiation [82]. This mechanism involves a dynamic process, wherein the activation of the surface of AuNPs by radiation-induced superoxides catalyzes the "conversion of intermediates to products" as exemplified by a 2000-fold increase in the yield of coumarin carboxylic acid hydroxylation.

Taken together, these studies provide evidence that AuNPs chemically enhance the effects of radiation by catalyzing radical reactions, and increasing the production of ROS. These highly reactive free radicals ultimately lead to radiation-induced cell kill by causing a cascade of ionization, and fixation of radiation-induced damage. Furthermore, chemical enhancement, as described herein, may also have biological consequences by exerting oxidative stress as a result of the elevated levels of intracellular ROS, which will be discussed in Section 2.3.1.

2.3. Biological enhancement

In the kV energy range, where photoelectric dose enhancement predominantly occurs (Refer to Section 2.1), AuNPs have emerged as a promising therapeutic strategy *in vitro* and *in vivo* (Tables 1 and 2). While kV radiation is used to treat patients with superficial tumors, it suffers from short penetration depth. Hence, most patients with deep tumors (e.g. cervical, pancreatic, prostate, brain) are commonly treated with MV radiation generated by a clinical linear accelerator (LINAC) to minimize excessive dose to skin. For this reason, radiosensitization at MV energies would be necessary to expand the clinical utility of AuNP radiosensitizers. However, based solely on physical dose enhancement, radiosensitization with AuNPs is expected to be insignificant at MV energies due to the minimal contribution of photoelectric absorption of photons. Indeed, theoretical predictions by Monte Carlo simulations calculated a DEF of 1.007–1.014 for 6 MV X-rays compared to 2.114 for 140 kV X-rays assuming 7 mg Au/g of tumor [83]. Interestingly, experimental studies using MV radiation showed dose enhancements that were significantly higher than estimated by modeling.

Experimental evidence of radiosensitization at the clinically relevant MV energies was first reported by Chithrani et al. who evaluated the dependence of radiosensitization on radiation energy (105 kVp, 220 kVp, 137-Cs (660 keV), 6 MV) [38]. As expected, a decrease in radiosensitization (DEF = 1.66 at 105 kVp, 1.43 at 220 kVp, 1.18 with 137-Cs) was observed with increasing energies, as a result of reduced contribution of the photoelectric-dependent dose enhancement. Surprisingly, a modest but significant dose enhancement was observed at the MV energy (DEF = 1.17). A similar trend was observed by Jain et al., in which DEFs of 1.41, 1.29 and 1.16 were achieved in MDA-MB-231 cells using 1.9 nm AuNPs (AuroVist™) in combination with 160 kVp, 6 MV, and 15 MV X-rays, respectively [43]. Since the early work with MV radiations, an increasing number of theoretical modeling [84–86] as well as *in vitro* [43,48,87,88] and *in vivo* [35,56] studies have demonstrated radiosensitization at the clinically relevant MV energies.

The discrepancies between theoretical predictions and experimental data open the door to the possibility of biological enhancement in addition to the physical mode of action. This was further supported by experimental evidence showing that AuNPs sensitize cells to bleomycin (SER = 1.38), a redox-active compound that induces cell kill via oxidative stress and DNA damage, validating the role of biological enhancement [43]. Based on the studies to date, three key biological pathways of radiosensitization have been identified: (1) oxidative stress, (2) cell cycle disruption, and (3) DNA repair inhibition. Although increasing evidence supports the biological contribution to radiosensitization, this effect appears to be strongly dependent on the particle parameters; and thus, the exact mechanism by which cells respond to biological stress exerted by AuNPs remains to be determined.

2.3.1. ROS production and oxidative stress

One of the primary pathways of radiation-induced cell killing is through the radiolysis of water, generating free radicals and ROS that interact with various cellular components [89]. ROS, including superoxide radicals (O_2^-), hydrogen peroxide and hydroxyl radicals ($^{\bullet}OH$), can cause cellular damage directly by interacting with biological molecules, or indirectly by exerting oxidative stress and triggering cell death via apoptosis or necrosis. As discussed in Section 2.2.2, AuNPs have been shown to induce the formation of ROS. The resulting oxidative stress has emerged as one of the central mechanisms of nanoparticle-induced cytotoxicity, in particular for inorganic and metallic nanoparticles, such as AuNPs [76,90–92].

In cellular systems, AuNP-induced elevation in intracellular ROS levels has been shown to elicit a multitude of biological effects that ultimately lead to cell death via apoptosis or necrosis. For example, Pan et al. examined the cellular response to 1.4 nm triphenylphosphine monosulfonate-capped AuNPs (Au1.4MS), and found that treatment with AuNPs was associated with increased ROS production and loss of mitochondrial potential, resulting in necrotic cell death [76]. Similar findings were reported by Cui et al. with a significant increase in intracellular ROS levels leading to necrosis observed in HeLa and L929 (fibroblast) cells following a 24 h exposure to 2.7 nm tiopronin-coated AuNPs [74]. In both studies, co-incubation of AuNPs with thiol-containing antioxidants, such as *N*-acetyl cysteine (NAC) and glutathione (GSH), neutralized the toxic oxidative effects of AuNPs, and restored cell survival. However, co-incubation with ascorbic acid, an antioxidant that lacks a thiol group, did not have an effect [76]. Based on these findings, it was proposed that the exposed surface of AuNPs not only promotes ROS generation, but also binds thiol-containing antioxidants through Au–S bond formation, which reduces the cellular redox capacity by depleting endogenous reducing agents. In addition to these studies, several reports have demonstrated cell death by apoptosis or necrosis through ROS generation using AuNPs with different sizes, shapes and surface properties [39,77–80].

The exact mechanism by which AuNPs trigger oxidative stress is not well understood. Nonetheless, it is believed to occur mainly through impairment in mitochondrial function as a consequence of elevated intracellular ROS. Wahab et al. reported that a dose-dependent increase in intracellular ROS levels induced by 10–15 nm citrate AuNPs was associated with an up-regulation of caspase 3 and 7, leading to apoptosis via mitochondrial dysfunction [77]. As well, Taggart et al. demonstrated that exposure to 1.9 nm AuNPs (AuroVist™) caused a decrease in mitochondrial membrane polarization and an increase in mitochondrial oxidation. The effects remained unchanged following 2 Gy irradiation (225 kVp), ultimately leading to apoptosis and radiosensitization [53]. Importantly, glucose-capped AuNPs were shown to increase radiation-induced ROS production in cells irradiated with 90 kVp and 6 MV X-rays, suggesting AuNP-induced oxidative stress as a viable mechanism of radiosensitization at both kV and MV energies [41].

As discussed above, a number of studies have demonstrated evidence in support of AuNP surface-mediated production of ROS that induces oxidative stress. Interestingly, a recent study demonstrated that the inhibition of proteins involved in the maintenance of cellular oxidative homeostasis may also lead to AuNP-induced oxidative stress. Liu et al. showed an increase in ROS levels via inhibition of thioredoxin reductase 1 (TrxR1) activity in cells incubated with tridecapeptide-capped Au_{25} clusters ($Au_{25}peptide_9$) [93]. TrxR1 is one of the major

regulators of the cellular redox environment in mammalian cells, and is also involved in cell viability and proliferation [94–99]. Due to its overexpression in many cancer cells, it has been actively sought out as a target for cancer therapy [100–102]. The specific binding of $Au_{25}peptide_9$ to the glutamic acid-rich domain of TrxR1 effectively suppressed its activity in a dose-dependent manner, causing a dramatic increase in intracellular ROS levels, and triggering cell apoptosis. To our knowledge, this is the only report on the inhibition of redox proteins by AuNPs; and thus, further studies are necessary to investigate this new avenue of AuNP-triggered oxidative stress.

Studies to date have provided ample evidence in support of AuNP-induced formation of ROS; however, the precise mechanisms leading to the biological enhancement of radiation effects remain to be elucidated. This emphasizes the need to determine the cellular responses to oxidative changes triggered by AuNPs, specifically in the context of radiosensitization.

2.3.2. Cell cycle effects

The cell cycle is one of the major determinants of cell sensitivity to radiation. While cells in late G2 and mitosis are the most radiosensitive, cells in late S phase are the most radioresistant [103]. As well, activation of cell-cycle checkpoints, that cause delays in the movement of cells through G1, S and G2 phases, is one of the main pathways of DNA damage response upon exposure to IR [104]. By preventing or slowing the progression of cells through the cell cycle, cells maintain genomic integrity by repairing radiation-induced damage or by activating cell death in the event of unsuccessful repair.

AuNPs have been shown to cause cell cycle disruption, an effect that is dependent on various factors including the physico-chemical characteristics of the nanoparticle as well as the cell line. El-Sayed's group investigated the cell cycle effects of nuclear-targeted AuNPs in a number of studies, and reported an increase in the sub-G1 population [105,106]. In particular, recent work in human oral squamous carcinoma (HSC-3) demonstrated that incubation with 30 nm NLS-AuNPs led to an increase in the cell population in the S phase and a decrease in the population in the G2/M phase. This in turn led to chemo-sensitization when combined with 5′-fluorouracil which is active in S phase cells [107]. Although these nanoparticles have not been studied in combination with radiation, additive effects are expected as a result of enhanced apoptosis.

Radiosensitization by AuNPs can also be achieved by inducing cell cycle arrest in the G2/M phase, which is known to be the most radiosensitive, as has been demonstrated by Roa et al. [52]. In this study, glucose-capped AuNPs (Glu-AuNPs, 10.8 nm) were shown to synchronize cells in the G2/M phase by inducing changes in the expression levels of cyclin kinases which are involved in the regulation of the cell cycle. Treatment with Glu-AuNPs led to an activation of cyclin B1 and cyclin E, and inhibition of p53 and cyclin A. Together, Glu-AuNPs sensitized prostate cancer cells (DU-145) to radiation (137-Cs) by causing acceleration through the G0/G1 phase and accumulation of cells in the G2/M phase, achieving DEFs as high as 1.38. Similar changes in cell cycle distribution were observed with Glu-AuNPs in ovarian (SKOV-3), breast (MDA-MB-231) and lung (A549) cancer cells, enhancing sensitivity to kV and MV X-rays [41,54,55], and with RGD-targeted gold nanorods (AuNRs) in melanoma cells [108].

In contrast to reports of cell cycle effects of AuNPs, there are also studies indicating no significant influence of AuNPs on cell cycle distribution [34,40,76]. For instance, Butterworth et al. reported cell line-dependent effects of 1.9 nm AuNPs (AuroVist™). Specifically, 48 h of exposure to AuNPs led to a significant increase in sub-G1 population in DU-145 cells, suggesting induction of apoptosis, this effect was not observed in MDA-MB-231 cells [34]. Lack of cell cycle effects by AuNPs was also reported by Pan et al. using 1.4 nm triphenyl monosulfonate-AuNPs [76], and by Cui et al. using 2.7 nm tiopronin-AuNPs [40]. Thus, further investigations are necessary in order to fully elucidate the effects of nanoparticle properties on perturbations in the cell cycle.

2.3.3. Inhibition of DNA repair

Upon exposure to IR, several types of DNA lesions, such as single strand breaks (SSBs), double strand breaks (DSBs), and DNA base modifications, are produced [109]. Among various types of DNA lesions, DSBs are considered to be most detrimental, and are shown to be correlated with clonogenic cell kill [110]. Correspondingly, the repair of DNA DSBs is essential in maintaining genomic stability, and the failure to successfully repair the damage leads to cell death via a number of pathways. Given the central role of DNA repair in cell survival, several cytotoxic agents that target DNA repair pathways, such as cisplatin, mitomycin C, and gemcitabine, have been investigated clinically to determine their potential as radiosensitizers [111]. As well, experimental analysis of DNA DSBs using the γ-H2AX foci assay, which detects one of the earliest events that occurs upon DSB formation [110], has identified DNA repair inhibition as a possible biological mechanism of radiosensitization by AuNPs.

Chithrani et al. found that incubation of HeLa cells with 50 nm citrate-AuNPs increased the number of γ-H2AX and 53BP1 foci at 4 and 24 h post-irradiation at both 220 kVp and 6 MV energies. Based on these findings, the increased residual damage in the presence of nanoparticles, indicative of delayed DNA repair, was suggested to be a key mode of radiosensitization [38]. Further evidence for AuNP-induced inhibition of DNA repair was provided by Cui et al., who reported a significant increase in the residual DNA damage (24 h post-IR) in cells irradiated with 250 kVp X-rays in the presence of 2.7 nm tiopronin-AuNPs, while no effect was seen on the initial (30 min post-IR) levels of DNA DSBs [40].

While some studies have demonstrated an inhibition of radiation-induced DNA damage repair with AuNPs, others have reported a lack of influence of AuNPs on DNA repair kinetics. For instance, Chen et al. showed that treatment of cells with BSA-capped AuNPs led to a 2.02- and 1.95-fold increase in the density of γ-H2AX foci at 2 and 4 h post-irradiation, respectively, as a result of the increased radiation-induced damage imparted by BSA-coated AuNPs. However, there was no difference in DNA DSBs after the incubation period (4–24 h), suggesting the absence of an effect of AuNPs on the DNA damage repair process [37]. In another study, cell exposure to 1.9 nm AuNPs (AuroVist™) had no influence on either DSB formation or repair, as demonstrated by the absence of an increase in the initial (1 h post-IR) and residual (24 h post-IR) number of γ-H2AX foci in MDA-MB-231 [43].

Considering the influential role of DNA repair in radiosensitization, inhibition of DNA damage response pathways appears to be a plausible mechanism of dose enhancement by AuNPs. However, discrepancies exist in the literature, and the involvement of AuNPs in DNA repair inhibition remains inconclusive. This warrants further studies to determine the precise role of AuNPs in various DNA repair pathways, and the contribution of particle properties (i.e. size, shape, surface chemistry), treatment conditions, as well as biological (i.e. cell line) and irradiation (i.e. dose rate, radiation source, dose, energy) parameters on radiation-triggered DNA damage response.

3. Recent advancements in AuNP radiosensitization

Early studies with AuNPs have focused on understanding the mechanisms and evaluating the feasibility of AuNP radiosensitization for applications in single modality RT. Despite the promising findings from pre-clinical studies, particularly in *in vitro* systems, the road towards clinical translation has proven to be challenging. One of the major barriers hindering the rapid clinical translation is the limited demonstration of therapeutic efficacy *in vivo*, specifically using clinically relevant MV radiation. In achieving a successful transition from *in vitro* to *in vivo*, AuNPs are faced with multiple challenges. For instance, many formulations require intra-tumoural injection to avoid aggregation and to achieve therapeutically relevant concentrations of Au at the tumor, limiting their clinical utility. As well, the concerns of long-term toxicity due to poor clearance of AuNPs from the liver are well

established. In order to overcome the limitations of first generation AuNP radiosensitizers, recent advancements have focused on developing strategies to further enhance the radiotherapeutic efficacy and to minimize long-term toxicities. By exploiting the synthetic versatility of AuNPs, actively targeted AuNPs as well as Au-based multifunctional nanoplatforms have been developed to enable multi-modal therapy and imaging. In addition, to further expand the clinical utility of AuNPs, their performance under clinically relevant scenarios (e.g. hypoxia, ion RT) have been evaluated.

3.1. Multi-functional AuNPs for multi-modal imaging and therapy

3.1.1. AuNP-induced hyperthermia

One of the unique features of AuNPs is their ability to absorb light due to local surface plasmon resonance (LSPR), which describes the collective oscillation of electrons induced by interaction with an electromagnetic field. Depending on the size and shape of the AuNPs, the LSPR wavelength can range from the ultraviolet (UV)-visible range to near-infrared (NIR). Specifically, the physical properties (e.g. shell thickness, size, aspect ratio) of Au nanorods and nanoshells can be engineered to fine tune the LSPR in the NIR (>800 nm), making them ideal for biomedical applications. The conversion of electromagnetic energy to thermal energy upon optical activation of Au nanoshells and nanorods can be utilized to cause direct anti-tumor effects via photothermal ablation or by inducing hyperthermia that sensitizes cells to chemo- and RT. In particular, mild hyperthermia is known to potentiate the effects of RT by increasing blood flow to mitigate tumor hypoxia, activating immunological responses, and modulating heat-related genes that influence DNA damage responses [112–115].

A number of techniques exist for delivering heat to generate hyperthermia, such as microwave, radiofrequency and ultrasound. AuNP-mediated heating provides unique benefits over these techniques, notably, their tumor targeting ability combined with radiosensitization and contrast enhancement properties that enable multi-modal applications. Indeed, AuNPs have been extensively studied for PTT [22,116–118], and also for combined treatment with RT to increase sensitivity to radiation and impart heat-associated cell damage. For example, Diagaradjane et al. showed that nanoshell-induced mild hyperthermia increased radiotherapeutic efficacy via two distinct mechanisms: (1) a reduction in the radioresistant hypoxic cell population as a result of an early increase in tumor perfusion, followed by (2) vascular disruption and necrosis as a result of localized thermal damage in the vicinity of the nanoshells, which are sequestered predominantly in the perivascular space [119]. In another study, folic acid-conjugated silica-modified Au nanorods (GNR-SiO_2-FA) were shown to increase radiation-induced clonogenic cell kill and heat-induced apoptotic cell death [32]. These nanoparticles also exhibited strong X-ray attenuation for *in vivo* X-ray and CT imaging, providing support for applications in image-guided RT and PTT.

To further enhance the tumor-specific targeting of hyperthermia and radiation, Hainfeld et al. devised a unique strategy that takes advantage of the aggregation-induced alteration in light absorption properties of AuNPs [120]. In this study, synergistic effects of hyperthermia in combination with RT were investigated using 15 nm spherical AuNPs that absorb NIR light upon reversible aggregation under acidic conditions. These nanoparticles, which have a mixed shell of PEG and the pH sensitive lipoic acid, are stable at physiological pH (pH 7.4) and absorb light in the visible region as individual particles. Upon exposure to the acidic tumor microenvironment (pH < 6.5) or under conditions of low endosomal (pH ~ 5.5) and lysosomal (pH 4–5) pH, the AuNPs undergo reversible aggregation, causing a red-shift into the NIR spectrum. In this study, upon intra-tumoural injection of the AuNPs, the tumors were heated to 48 °C for 5 min, followed by irradiation with 100 kVp X-rays (average time between heating and irradiation: 3 min, 9 s). Treatment with AuNPs in combination with NIR and IR (15, 20, 25 Gy) resulted in significant radiosensitization, reducing the tumor control dose by a factor of 3.7, and improving the long-term (>250 days) survival rate from 33% with IR alone to 71% with the triple combination. This strategy provides multiple advantages over classical AuNP-based radiosensitization, namely, the unique aggregation behavior that increases tumor residence time of the AuNPs, and confines heating specifically to the tumor regions wherein the AuNP aggregates have localized, limiting the radiation dose to normal tissues.

While the AuNP-based heating method offers unique potential for multi-modal therapy in combination with RT, there are challenges to be overcome, namely, the limited penetration depth of NIR light source used for heat activation. Due to this limitation, application of this technology is restricted to superficial tumors or those that are easily accessible. This must be taken into consideration when designing a AuNP-based platform for combined PTT and RT.

3.1.2. Hybrid nanoplatforms of AuNPs

The size of AuNPs is one of the key physico-chemical properties that influences their cellular and *in vivo* fate, which in turn, dictates the performance of AuNP-based therapy. While large AuNPs (> 10 nm) enable exploitation of the EPR effect for tumor accumulation, they are limited by poor intra-tumoural penetration in addition to relatively high uptake in the liver and spleen, raising concerns of long-term toxicities and immunogenic response. On the other hand, small AuNPs (<~7 nm) provide benefits of enhanced tumor penetration and reduced recognition by the reticulo-endothelial system (RES); however, they undergo rapid renal clearance, limiting tumor accumulation and retention which are both necessary for contrast enhancement and radiosensitization. In addition to the highlighted differences, other properties, such as cell uptake and cytotoxicity, vary greatly with AuNP size, further complicating the selection of particle parameters ideal for biomedical applications. One approach to overcoming the size dilemma with AuNPs is to combine the best of both worlds by generating hybrid systems that encapsulate small AuNPs in a larger nanoparticle platform, commonly micelles or liposomes, to maximize control over the particle's *in vitro* and *in vivo* properties (e.g. intracellular distribution, pharmacokinetics). This strategy also provides an opportunity for multi-modal treatment by packaging AuNPs with other imaging or therapeutic agents. Although limited reports have evaluated the effectiveness of hybrid nanoparticles for Au-based radiosensitization, the results to date provide promising potential for further development.

In a recent study, Yang et al. prepared amphiphilic AuNPs that included an organic shell consisting of hydrophilic 11-mercaptoundecanesulfonate (MUS) and hydrophobic octanethiol ligands, which enable cell membrane penetration [121]. These AuNPs were embedded in the lipid membrane of interbilayer-crosslinked multi-lamellar lipid vesicles to form Au nanocapsules (AuNCs). Analysis of the intracellular distribution of the AuNCs demonstrated initial internalization in endosomes with the amphiphilic AuNPs distributed in the cytosol and cellular membrane following endosomal escape. When combined with RT, the increased homogeneity of nanoparticle distribution via cytosolic dissemination of AuNPs in B16F10 melanoma led to a 3-fold increase in radiation-induced clonogenic cell kill compared to irradiation alone.

In another study, Tsourkas' group took advantage of the multifunctional properties of Au as a CT contrast agent as well as a radiosensitizer to develop Au-loaded polymeric micelles (GPMs) that contain 1.9 nm AuNPs in the hydrophobic core of the micelles formed from a poly(ethylene glycol)-*b*-poly(ε-caprolactone) copolymer (PEG-*b*-PCL) [122]. Compared to the commercially available 1.9 nm AuroVist™ nanoparticles, which do not provide significant contrast enhancement due to rapid renal clearance ($t_{1/2}$ = 30 min), GPMs exhibited a longer circulation half-life ($t_{1/2}$ = 1 h in early distribution phase, $t_{1/2}$ = 8.7 h in elimination phase), resulting in a 6-fold increase in tumor accumulation (6.2 ± 1.2% ID/g for GPMs vs. 1.0 ± 0.1% ID/g for AuroVist™) and improved tumor visualization. At 24 and 48 h post-administration, GPMs were found to be heterogeneously distributed in the tumor periphery

enabling tumor margin delineation to guide radiation delivery. In combination with RT, treatment with GPMs radiosensitized human fibrosarcoma (HT1080) cells both *in vitro* and *in vivo*, resulting in a DEF of 1.2, and a 1.7-fold increase in median survival time (68 days) compared to mice treated with radiation alone (38 days). The findings of this study provided promising evidence for the application of GPMs in image-guided RT. However, the GPMs suffered from the low sensitivity of CT imaging, which requires delivery of significantly higher concentrations of Au to the tumor to generate sufficient contrast enhancement in CT (mM range) relative to the amount necessary for radiosensitization (μM range).

To overcome the limitations of Au-based CT imaging, the same group reported a second-generation micelle-based nanoplatform that encapsulates both AuNPs for RT and SPIONs (superparamagnetic iron oxide nanoparticles) for highly sensitive MR imaging (Gold- and SPION-loaded polymeric Micelles, GSMs) [123]. The tumor accumulation of GSM (6.64% ID of Au or Fe/g tumor) generated a hypointensive signal in MRI, while no significant contrast enhancement was seen in CT. As well, X-ray irradiation (6 Gy; 150 kVp) following GSM administration and imaging led to a significant radiosensitization effect, resulting in a statistically significant increase in mean survival (75.6 ± 9.2 days) relative to the irradiation only group (50.4 ± 10.6 days).

Therefore, the integration of AuNPs into other nanoplatforms (e.g. liposomes, micelles) produces multifunctional nanoparticles with unique properties that cannot be achieved with AuNPs alone. This strategy holds promising potential in developing versatile AuNP-based nanoplatforms that are capable of multi-modal diagnostic and therapeutic applications.

3.1.3. AuNP-drug conjugates

As discussed in the introduction, AuNPs provide an ideal platform for tumor-targeted drug delivery owing to their well-established synthetic versatility. The delivery of chemotherapeutic agents using AuNP-drug conjugates offers multiple advantages over free drug administration, including enhanced tumor specificity via passive or active targeting, increased tumor bioavailability by minimizing drug inactivation, and the flexibility for combined treatment with other therapeutic or imaging modalities. Given this range of beneficial features, a number of AuNP-based therapeutic platforms have been developed for anti-cancer applications as highlighted in recent reviews [27,124,125].

Further therapeutic gains can be achieved by using AuNP-drug conjugates in combination with RT by applying the principles of concurrent chemo-RT. Clinically, chemo-RT is utilized to improve treatment outcome via (1) spatial cooperation, (2) independent cell kill, or (3) cellular and molecular interactions [1,126]. In particular, concomitant administration of chemotherapy has been shown to significantly enhance tumor response, and ultimately the loco-regional control, by potentiating the effects of RT [127]. A number of chemotherapeutic agents have been clinically investigated for chemo-RT [126,128,129]. In particular, cisplatin has been shown to exhibit radiosensitization effects through various mechanisms, including enhanced formation of toxic platinum intermediates, cell cycle disruption, activation of apoptosis, inhibition of DNA repair, and fixation of IR-induced DNA damage [127,130–133]. Clinically, cisplatin-based concurrent chemo-RT is the standard treatment for locally advanced cervical cancer, squamous cell carcinoma of the head and neck, and non-small cell lung cancer. However, cisplatin-related toxicities, namely, hematologic and renal toxicities as well as neuropathy, remain the major challenges limiting the efficacy of platinum-based chemo-RT regimens. The limitations of dose-limiting systemic toxicities can be overcome by improving tumor targeting via conjugation to AuNPs. As well, a study with plasmid DNA demonstrated that the binding of two cisplatin molecules and one AuNP to DNA drastically enhances radiation-induced DSB formation by a factor of 7.5 [134]. The synergistic effects were attributed to the combination of the AuNP-induced increase in LEEs and the formation of transient cisplatin anions that enhance electron capture in the DNA, weakening the bond at the site of cisplatin. Taken together, these findings provide a strong rationale for developing an AuNP platform of cisplatin for chemo-RT applications.

In a proof-of-concept study by Lee et al., cisplatin-conjugated AuNPs were generated via complexation of cisplatin to the carboxylate groups of poly(acrylic acid)-capped AuNPs (>1300 Pt^{II} per AuNP), and their chemotherapeutic potency, as well as secondary electron emission were investigated [135]. *In vitro* analysis revealed that the drug activity remained unaffected by the complexation process, demonstrating comparable cytotoxicity to free cisplatin. As well, upon irradiation with non-monochromated Bremsstrahlung radiation, a kinetic energy spectrum that corresponds to the Auger electron emission lines of Pt and Au was observed confirming the release of low energy secondary electrons. In another study, Setua et al. used a pH-sensitive coordination bond to tether cisplatin to mercaptoundecanoic acid (MUA)-capped Au nanospheres, which activated γ-H2AX foci formation, and decreased the cell growth rate compared to the control or cells treated with MUA-AuNPs. In combination with 10 Gy γ-rays (137-Cs), the authors observed radiosensitization effects accompanied by an increase in caspase 3-mediated apoptosis, resulting in growth delay and the complete ablation of patient derived GBM cells *in vitro* [136]. In this study, AuNP-Pts were localized in the cytosolic vesicles, and were not observed in the nucleus, hence, the synergistic dose enhancement effects as proposed by Sanche et al. could not be exploited. Nonetheless, the combination of cisplatin cytotoxicity and Au/Pt-mediated radiosensitization led to improved therapeutic effects compared to RT alone.

In addition to cisplatin, doxorubicin (DOX) has also been shown to enhance DNA DSBs when combined with ionizing radiation [137]. AuNP-mediated chemo-RT with DOX has been explored through use of AuNPs to deliver DOX specifically into cancer cells and in one study, with drug availability ensured by X-ray triggered release. For example, Zhou et al. demonstrated that DOX-loaded dual-targeting AuNPs caused significantly greater DNA DSBs compared to free DOX upon X-ray irradiation, which corresponded to a 2.7-fold increase in cell killing [138]. The enhanced cell killing was attributed to the combined effects of AuNP radiosensitization and DOX cytotoxicity, exerting a “double assault” on the DNA target. In another study, X-ray irradiation was shown to trigger the release of DOX from DOX-conjugated DNA-coated AuNPs (DOX-DNA-AuNPs) [139]. The increased cellular bioavailability of DOX enabled drug diffusion into the nucleus exerting DNA damage and resulting in a greater clonogenic cell kill compared to DOX-free DNA-AuNPs.

3.1.4. All-in-one AuNP formulation

The examples discussed above have demonstrated the potential of AuNPs as a versatile nanoplatform for dual-modality imaging and therapeutic applications. To add another layer of complexity, the unique synthetic and electronic properties of AuNPs can be further exploited to develop an all-in-one multi-functional nanoplatform that facilitates triple combination therapy (i.e. chemo, radio, thermal therapy) in addition to CT-imaging capabilities. In particular, hollow AuNPs (HGNPs) provide an ideal platform for multi-functional applications due to their unique optical and morphological properties. The Au shell not only enables radiosensitization and CT contrast enhancement, but the shell thickness can also be fine-tuned for photothermal ablation using NIR light. As well, the hollow cavity can be utilized to encapsulate high loading of therapeutic agents for chemotherapy. Exploiting the multifunctional characteristics of HGNPs, Park et al. evaluated the therapeutic potential of DOX-loaded HGNPs (DOX-HGNPs) for combined chemo-, radio- and thermal therapy [140]. As discussed above, it is well-established that hyperthermia sensitizes cells to chemo- and RT. Additionally, DOX has shown additional benefits in combination with RT [137]. Taken together, synergistic effects were expected using this therapeutic strategy. Indeed, the triple combination group (i.e. DOX-HGNPs + NIR + 6 MV X-rays) was shown to result in a 4.3-fold increase in tumor growth delay, as well as a 6.8-fold reduction in tumor weight

compared to the control mice. The dramatic anti-tumor effects were attributed to the NIR-triggered release of DOX (4-fold increase with NIR) in combination with the enhanced tumor response to chemo- and RT at elevated temperatures (~45 °C). In addition to the therapeutic benefits, DOX-HGNPs were shown to result in a 5.3-times higher CT attenuation coefficient in comparison to Ultravist 300, an iodine-based CT contrast agent that is widely used in the clinic, demonstrating promising potential for combined image-guided thermal and RT.

3.2. Actively targeted AuNPs

Studies evaluating the factors that influence radiosensitization have identified the intracellular concentration and localization of AuNPs as the major determinants of radiation enhancement [38,47]. These findings highlight the necessity to optimize the particle properties in order to maximize cellular uptake for radiosensitization. One of the commonly employed approaches to increase the cellular binding and uptake of AuNPs, ultimately improving the radiotherapeutic efficacy, is to introduce cancer cell-specific targeting ligands to the surface of the particles [40,141–147].

Khoshgard et al. compared the radiosensitizing effects of folate-conjugated and non-conjugated AuNPs in HeLa cells that express high levels of the folate receptor [46]. A significantly higher dose enhancement effect was achieved upon exposure to 180 kVp X-rays with folate-conjugated (DEF = 1.64 ± 0.05) versus non-conjugated (DEF = 1.35 ± 0.05) AuNPs, which was attributed to the 6-fold higher cellular uptake of the targeted nanoparticles compared to their untargeted counterpart. In addition, targeting the epidermal growth factor receptor (EGFR) has been shown to significantly increase the cellular uptake of Au nanospheres compared to non-targeted nanospheres. When combined with 6 MV X-rays, a significant increase in cell killing (70.54% SF with non-targeted vs. 54.28% SF with EGFR-targeted AuNPs) was achieved as a result of cell cycle arrest and increased apoptosis via down-regulation of anti-apoptotic Bcl-2 and up-regulation of pro-apoptotic Bax, Bad and caspase 3 [87]. As well, Wolfe et al. used goserelin-conjugated Au nanorods (gAuNRs) that target the luteinizing hormone-releasing hormone (LHRH) receptors, which are over-expressed in many prostate cancers, to sensitize PC3 cells to 6 MV X-rays, achieving DEFs of 1.36 with the targeted gAuNRs and 1.19 with the non-targeted PEG-AuNRs [56]. *In vivo*, treatment with gAuNRs in combination with 5 Gy, 6 MV RT resulted in a significant delay in tumor regrowth (17 ± 1 days) compared to RT alone. In another study, HER2-targeting with trastuzumab resulted in cell-specific uptake of 15 nm AuNPs *in vitro*, and an enhancement in CT contrast *in vivo*, in particular within the tumor periphery [145]. In combination with X-rays, HER2-targeting enabled efficient transport of AuNPs into the HER2-overexpressing SK-BR3 cells, and caused a 5.1-fold increase in DNA DSBs compared to irradiation alone [148].

In addition to targeting cell surface receptors that are commonly over-expressed in cancer, the metabolic characteristics of cancer cells can be exploited to enable cancer-specific uptake of AuNPs. In order to support rapid uncontrolled growth, cancer cells exhibit higher glucose demand compared to normal cells. The differences in cellular glucose uptake is the basis of employing fluoro-deoxyglucose (FDG) as a functional metabolic imaging probe in positron emission tomography (PET), and the same principles can be applied to enrich cancer cell-specific uptake of glucose-coated AuNPs (Glu-AuNPs). Glu-AuNPs have shown 10–100 times greater uptake in cancer cells compared to normal cells, resulting in cancer cell-specific radiosensitization in breast (MCF-7) and prostate (DU-145) cells using kV radiation [47,52]. Successful radiosensitization was also observed using 6 MV X-rays [41,54,55], 60-Co γ-rays [45], and carbon ions [45]. *In vivo*, the administration of PEGylated Glu-AuNPs prior to RT significantly inhibited tumor growth compared to RT alone in murine models of breast [149] and cervical cancer [150].

3.3. AuNPs as hypoxic radiosensitizers

Tumor hypoxia, which bears clinical implications on treatment outcome, is one of the major challenges in the treatment of cancer [151,152]. In the context of RT, radioresistance of hypoxic cells confers an increased risk of tumor recurrence and poor prognosis [153,154]. Oxygen is a key mediator of radiation response owing to its role in chemically fixing the radiation-induced cellular damage [155]. Upon exposure to IR, DNA damage is inflicted via direct interactions with photons or through the indirect action of radicals formed from the radiolysis of water. In the presence of oxygen, free radicals generated at the DNA react rapidly with oxygen to generate permanent damage, whereas under hypoxic conditions, the radicals have a longer half-life and can undergo restitution to chemically restore the DNA. The diminished oxygen effect, under hypoxic conditions, reduces the efficacy of RT, necessitating therapeutic strategies to enhance the radiation effects.

While early studies with AuNPs have been limited to normoxia, recent investigations have also evaluated their potential under hypoxia. Cui et al. evaluated the cellular uptake and radiosensitization effects of 2.7 nm tiopronin-coated AuNPs under normoxia (21% O_2) as well as acute (4 h in 0.2% O_2) and chronic (72 h in 0.2% O_2) hypoxia [40]. In this study, two different hypoxic conditions were tested to mimic the clinical solid tumor, wherein both perfusion- (i.e. acute) and diffusion-limited (i.e. chronic) hypoxia exist. In acute hypoxia, cells close to blood vessels undergo cycles of hypoxia and re-oxygenation, whereas cells far from blood vessels experience chronic hypoxia, which can last from hours to days. A three-fold higher intracellular level of Au was observed in cells under normoxia compared to those under chronic or acute hypoxia. *Superior* radiosensitization by AuNPs was observed under normoxia, which was followed by chronic and acute hypoxia. The greater radiosensitizing effect of AuNPs in cells under chronic (SF ratio = 0.22 ± 0.08) compared to acute hypoxia (SF ratio = 0.61 ± 0.07) was attributed to the established reduction in activity in the homologous recombination repair pathway under chronic hypoxia. As well, exposure of cells to oxygen prior to irradiation (i.e. irradiation of hypoxic cells under normoxic conditions) restored the radiosensitization effects of AuNPs, highlighting the crucial role of oxygen in AuNP-mediated radiation enhancement.

In another study, Jain et al. reported radiosensitization using 1.9 nm AuNPs (AuroVist™) under normoxia (21% O_2, DEF = 1.41) and moderate hypoxia (1% O_2, DEF = 1.39); however, no significant sensitization was observed under near anoxia (0.1% O_2, DEF = 1.1) [42]. Reduced radiosensitization under near anoxia was attributed to a decrease in the cellular uptake of AuNPs via receptor-mediated endocytosis (RME) due to a switch from aerobic to inefficient anaerobic energy production under these conditions.

In both studies, reduced radiosensitizing effects of AuNPs were observed under various hypoxic conditions relative to normoxia. Nonetheless, significant radiosensitization was still achieved, which provides promising support for clinical utility of AuNPs.

3.4. Radiosensitization with proton and carbon RT

While the majority of studies to date have focused on the use of AuNP radiosensitizers with photons (i.e. X-rays and γ-rays), there has been a growing interest in expanding their application to other radiation sources, such as protons and heavy ions (e.g. carbon). In contrast to photon RT, in which maximum dose deposition occurs near the body surface as the beam enters tissue, ions penetrate through the tissue with relatively low energy transfer until they reach the Bragg peak. Maximum dose deposition at the Bragg peak is followed by a steep decrease at the end of range, enabling more conformal localization of radiation dose. Given the unique depth-dose profile of proton and heavy ions (e.g. C^{6+}, Ne^{10+}, Si^{14+}, Ar^{18+}), a more favorable dose distribution is achieved with ion RT relative to photon RT, sparing normal tissues from radiation-induced toxicities. As well, for high linear energy

transfer (LET) radiation (e.g. heavy ions, neutron), which deposits dose at higher densities compared to low-LET radiation (e.g. X-rays, γ-rays, electrons), there are additional biological benefits. These benefits include lower sensitivity to oxygen-based resistance, reduced dependence on cell cycle distribution, and a narrower range of radiation response, rendering high LET radiation ideal for slow-growing and X-ray-resistant tumors, as well as highly hypoxic tumors [1]. Given these advantages, in particular for treatment of pediatric cancer and deep-seated tumors (e.g. prostate, inoperable lung cancer) [156–158], there has been a dramatic growth in the clinical implementation of ion RT, in particular for proton therapy [159].

Although limited literature exists, recent studies have demonstrated the feasibility of using AuNPs to radiosensitize cells to proton and carbon RT. For example, Kim et al. demonstrated a 90% reduction in tumor volume upon administration of 300 mg/kg AuNPs in mice bearing CT26 mouse colorectal adenocarcinoma followed by irradiation with 45 MeV protons, whereas irradiation alone showed only an 18% reduction followed by tumor regrowth [160]. Long term survival studies reported by the same group in a subsequent publication demonstrated that the one-year survival of mice increased from 11 to 13% with proton therapy alone to 58–100% with the addition of AuNPs, which was attributed to the enhancement of ROS generation [161]. In another study, Polf et al. reported a 15–20% increase in relative biological effectiveness (RBE) of proton RT (160 MeV) by internalized AuNPs in DU145 prostate cancer cells [162]. Using carbon ions, Kaur et al. showed a 29% dose reduction and 41% increase in RBE in cells treated with 62 MeV $^{12}C^{6+}$ irradiation in the presence of Glu-AuNPs compared to those without AuNPs [45]. Radiation enhancement effects of AuNPs using carbon ions (165 MeV) were also demonstrated by Liu et al., in which a maximum DEF of 1.44 was achieved, which was proposed to be a result of increased production of hydroxyl radicals [50].

In order to understand the mechanism underlying sensitization to proton therapy, theoretical calculations have been performed by Lin et al. [163,164]. Monte Carlo simulations demonstrated that while similar doses are deposited in the nanometer vicinity of the particles, the longer range secondary electrons produced by kV photons resulted in a much greater dose deposition at micrometer distances by kV photons compared to protons [163]. Due to the short range of secondary electrons generated by AuNPs irradiated with protons, particle localization in close proximity to the cellular target is particularly important in proton therapy. In a subsequent publication, the same group applied the Local Effect Model to describe the biological effects and compare the survival of cells irradiated with photons and protons in the presence of AuNPs [164]. In this study, it was revealed that the intracellular AuNPs, specifically those localized within the nucleus, contributed most significantly to radiosensitization. Comparing the three irradiation modalities (i.e. kV photons, MV photons, protons), greatest enhancements were calculated for kV photons due to the highest probability of interaction with AuNPs. For proton irradiation, a reduced sensitizer enhancement ratio (SER) of 1.33 was obtained assuming intracellular concentration of 1 μM AuNPs, which was further increased to 1.81 assuming nuclear localization, once again illustrating the importance of cellular and nuclear uptake of AuNPs for proton radiosensitization. Although there are limitations to this approach, notably, the simplified cell geometry, and the confinement of radiation dose to the nucleus (i.e. damage to non-DNA targets was not considered), findings of this study confirms the feasibility of AuNP radiosensitization with proton RT given sufficient Au deposition in close proximity to the nucleus.

While considerable dose enhancements have been observed using protons of high energies (> 50 MeV), at lower energies, radiosensitization effects of AuNPs were reported to be insignificant or less pronounced compared to those at higher energies. For instance, *in vitro* studies by Liu et al. demonstrated a 2–11.9% decrease in the clonogenic cell survival rate with PEGylated AuNPs in combination with 3 MeV proton therapy, which the authors described as a "weak but still detectable radiation enhancement effect" [48]. As well, a recent study by Jeynes et al. showed no significant difference in the surviving fractions of RT112 bladder cancer cells treated with 5 Gy, 3 MeV protons with or without 50 nm AuNPs. The addition of a free radical scavenger had no protective effect in proton-irradiated cells, suggesting that ROS is not the major source of cellular damage imparted by low energy protons. Based on these findings, the authors postulated that the lack of observed radiosensitization by AuNPs with low energy protons is due to the difference in energy and the corresponding LET of the ions interacting with nanoparticles. High energy protons with LET below 5 keV/μm exhibit a higher probability of colliding with AuNP-containing vesicles compared to that of low-energy protons with higher LET (above 10 keV/μm) [165]. Additionally, since the energy of the secondary electrons emitted is dependent on the energy of the primary ion, a greater number of secondary electrons will escape the nanoparticle to impart cellular damage upon interaction with high-energy protons compared to low-energy protons.

Overall, theoretical and experimental evidence obtained to date provide an encouraging outlook for the use of AuNP radiosensitizers in ion RT, in particular for proton therapy. However, this therapeutic strategy is still in its infancy, and further understanding of the mechanism underlying the energy-dependent radiosensitization by AuNPs will be necessary.

4. Design of ideal AuNPs for RT

Since the initial report by Hainfeld et al. [33], multi-disciplinary research that spans from radiation physics, biology and chemistry to formulation sciences has resulted in an extensive growth in the field of AuNP-based radiosensitization. Despite the promising findings of preclinical studies, clinical translation has proven challenging. To date, two nanoparticle formulations of Au have been clinically investigated for cancer treatment: (1) CYT-6091 (recombinant human tumor necrosis factor alpha (rhTNF)-bound PEGylated colloidal AuNPs) for the delivery of rhTNF (clinicaltrials.gov, NCT00356980, NCT00436410), and (2) AuroShell® (silica core-Au shell nanoparticles) for photothermal ablation in head and neck (clinicaltrials.gov, NCT01679470) and lung cancers (clinicaltrials.gov, NCT01679470). The results of Phase I clinical trials with CYT-6091 reported tumor-targeted delivery of Au and no major dose-limiting toxicities [166]. Currently, Phase II clinical trials with CYT-6091 in combination with standard of care second line therapy are being pursued for the treatment of non-small cell lung cancer. These developments provide promising evidence for the potential clinical translation of AuNPs; however, clinical evaluation of AuNPs for radiosensitization applications has not yet been pursued.

One of the barriers hindering the clinical translation of AuNPs for RT is the limited *in vivo* demonstration of their radiotherapeutic effect. A large number of theoretical and experimental studies involving plasmid DNA and cellular systems have demonstrated the radiosensitization potential of AuNPs. While significant progress has been made *in vitro*, translating the *in vitro* success to *in vivo* has been challenging. As well, many formulations lack colloidal stability, requiring intra-tumoural injection to minimize the adverse effects of particle aggregation, and to ensure sufficient Au concentration at the tumor site. Another major hurdle in the clinical translation of AuNPs is the possible long-term toxicities that may arise due to associated prolonged retention of the particles in the liver.

In order to improve the clinical utility of AuNP radiosensitizers, it is essential to identify the factors that influence the *in vivo* radiation enhancement effects of AuNPs, and incorporate these features in formulation design. Due to the wide variations in particle properties (e.g. size, shape, surface coating, functionalization), cell lines and radiation energies used to date, it is challenging to draw definitive conclusions on the major determinants of AuNP radiosensitization. Nonetheless, mechanistic studies have identified a number of key particle parameters that dictate the *in vivo* performance of AuNPs. In addition to the factors that are applicable to many nanoparticle systems in general (e.g. long

circulation lifetime, tumor accumulation, penetration), particular emphasis must be placed on colloidal stability, cellular and nuclear localization, as well as clearance in order to improve the radiotherapeutic efficacy and toxicity profile of AuNPs. These factors are highly dependent on the size, shape and surface properties of AuNPs [167–170]; and thus, efforts should be dedicated to tailoring nanoparticle properties to obtain AuNPs with ideal characteristics for radiotherapy.

By following the journey of a AuNP from intravenous injection to clearance, critical features and design considerations are now discussed (Fig. 4). Upon introduction into the blood stream, AuNPs are susceptible to interactions with the complex biological environment that includes high concentrations of ions and proteins as well as other blood components. Interactions with molecules in biological media may destabilize the particle surface by disrupting the electrostatic repulsive forces, favoring van der Waals attractions between particles that result in aggregation [171]. For instance, exposure to solutions of high osmolarity has been shown to reduce the colloidal stability of AuNPs, visibly evident by a red shift (i.e. color change from red to blue) and broadening of the SPR band [172,173]. In addition, AuNPs undergo ligand exchange with thiol-containing biomolecules (e.g. glutathione, cysteine), which may also induce aggregation. Irreversible aggregation of AuNPs in the circulation not only alters the cellular (e.g. uptake, toxicity) responses [174] and the pharmacokinetic (PK) profile of the nanoparticles, but it may also lead to adverse events such as blockage of blood vessels. Another factor that affects the *in vivo* fate of AuNPs is the non-specific binding of proteins to the particle surface. Depending on the physico-chemical properties of nanoparticles (e.g. surface chemistry, curvature, size), serum proteins are adsorbed to form a protein corona [175]. While some studies have demonstrated increased colloidal stability upon protein adsorption [176,177], the formation of protein corona may induce particle aggregation via protein-protein interactions [178]. For these reasons, it is critical that AuNPs exhibit high colloidal stability to enable intravenous administration.

Once in the blood stream, stable AuNPs must have sufficiently long circulation lifetime in order to exploit the EPR effect and preferentially accumulate at the tumor site. As the long circulating nanoparticles extravasate from the tumor vasculature, they must penetrate the tumor interstitium in order to achieve homogenous distribution of AuNPs. Penetration is also necessary to reach hypoxic cells, which are highly radioresistant and are generally distant from the vasculature albeit acute hypoxia may occur in proximity to the vessels. Among various particle parameters, size is a major determinant of tumor penetration. As expected, smaller AuNPs have demonstrated advantages in achieving homogeneous intra-tumoural distribution compared to larger particles, which have been shown to localize predominantly in the periphery of multi-cellular tumor spheroids (MCTS) [179,180].

Upon tumor accumulation and penetration, cellular localization is necessary to achieve effective radiosensitization. A number of studies have shown that the intracellular AuNPs contribute significantly to dose enhancement, whereas the extracellular or membrane-bound particles do not cause significant radiosensitization [38,40,47], clearly demonstrating the need for cellular internalization of AuNPs. Cellular uptake of AuNPs occurs predominantly through receptor-mediated endocytosis (RME), which is an energy-dependent process that is highly influenced by the particle size and shape, as well as the degree of non-specific adsorption of serum proteins [181,182]. In addition to the optimization of particle parameters, targeting moieties (e.g. antibodies, peptides) can be appended to the particle surface to further enhance cancer cell-specific uptake of AuNPs. While cytoplasmic localization of AuNPs is sufficient to yield radiosensitization, nuclear penetration

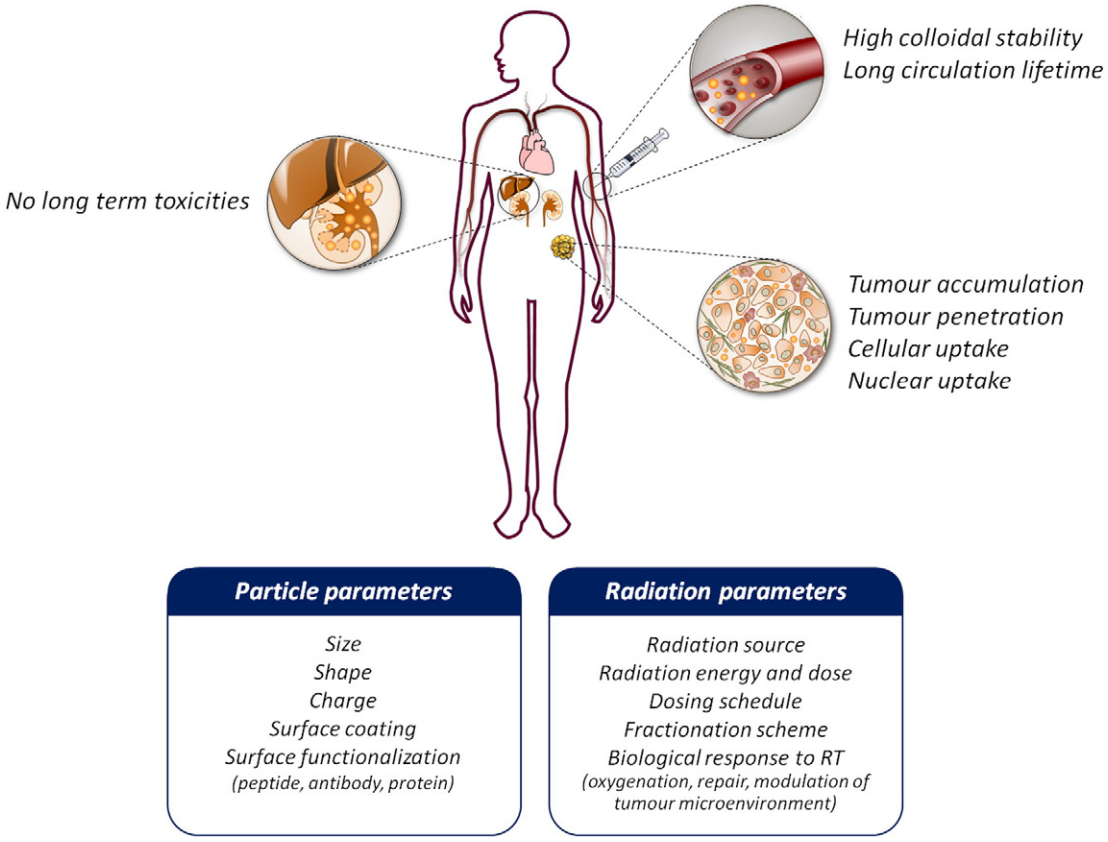

Fig. 4. Ideal characteristics of AuNPs. The physico-chemical properties of AuNPs can be optimized to obtain stable, long-circulating particles that preferentially accumulate in the tumor. Following extravasation and penetration into the tumor interstitium, these AuNPs must enter the tumor cells, and preferably the nucleus, where they radiosensitize these cells via physical, chemical and biological enhancements. Upon tumor-specific enhancement of radiation effects, these particles must be eliminated without causing long-term toxicities to the liver. In addition to the particle properties, radiation parameters can be tailored to exploit the biological response to radiation.

enables additional DNA damage via physical dose enhancement by the short-range LEEs [65,66,85,183,184], and chemical enhancement by the very LEEs [67,68]. As well, nuclear accumulation introduces the possibility to exploit synergistic combinations of AuNPs and a chemotherapeutic agent, such as cisplatin [134]. Upon cellular entry via the RME, AuNPs are confined within the lysosomes and endosomes. Consequently, AuNPs must either escape the endosomes, or utilize a different pathway of cell uptake (i.e. bypass RME) in order to achieve nuclear translocation. As well, nanoparticles must be smaller than 30 nm in size to allow importation through the nuclear pore complex [185]. Successful nuclear localization via endosomal escape has been reported using AuNPs that are modified with one or more cell-penetrating (e.g. Tat peptide) or nuclear-localizing (e.g. nuclear localization signal (NLS)) peptides, which are rich in positively-charged residues (e.g. lysine, arginine) [185–194]. However, the radiosensitization effects of these nuclear-targeting particles have not been evaluated. Inside the cell, and preferably the nucleus, AuNPs can exert radiosensitization effects through multiple pathways as discussed in Section 2. Although the impact of physico-chemical properties on different mechanisms of radiosensitization have not been studied extensively, size has been shown to affect the pathways of radiosensitization. Small AuNPs have been found to be more catalytically active; and thus, generate more ROS and induce greater cytotoxicity compared to larger particles [73,74,76,195]. As well, studies with plasmid DNA using kV radiation showed greater chemical enhancement with small, positively charged AuNPs relative to the large, negatively charged particles as a result of tight binding to DNA [68].

Upon the arrival of AuNPs at their target destination (i.e. tumor), another critical factor to be considered is clearance. Two recognized pathways of AuNP elimination are through the kidneys and liver. While small AuNPs (i.e. <~7 nm) are rapidly eliminated via renal clearance, larger AuNPs (i.e. 10–100 nm) accumulate in the liver and spleen via opsonization followed by recognition by the RES. A number of studies have reported that AuNPs reside in Kupffer cells in the liver for a period of time ranging from days to even months following intravenous injection [196–203]. In particular, Sadauskas et al. reported that only 9% of 40 nm citrate-AuNPs in the liver were cleared over 6 months, demonstrating the slow hepatic elimination of AuNPs [197]. Long-term retention of AuNPs in the liver has been shown to elicit a wide range of adverse effects, including histological alterations [198,199], changes in gene expression [200], and secretion of inflammatory cytokines, resulting in apoptosis [201–203]. To minimize long-term toxicities induced by AuNPs, efforts should be dedicated to tailoring nanoparticle properties to enable renal clearance, or to reduce opsonization and clearance by Kupffer cells.

Taking these factors into consideration, optimization of particle parameters is critical in developing the next generation of AuNP radiosensitizers that encompass the aforementioned ideal features. It is clear that these features cannot be achieved with AuNPs alone as a single modality platform. As such, another viable strategy is to develop multi-functional nanoplatforms that enable flexible manipulation of their *in vitro* and *in vivo* properties. This approach would also allow theranostic or multi-modal therapeutic applications by combining the radiosensitization effects of Au with imaging, thermal and drug delivery capabilities of AuNPs as discussed in Section 3. In addition to particle modification, other factors such as radiation energy, fractionation scheme, and the biological responses to radiation (e.g. vascular changes, oxygenation, repair kinetics) can be tailored to further improve the *in vivo* performance of AuNPs.

In this review, discussion of the radiosensitization effects of AuNPs was largely limited to EBRT using X-rays at high and low radiation energies. Other radiation factors, such as the radiation dose, dose rate, fractionation scheme, and radiation source, also play a critical role in determining the tumor response to radiation. For instance, dose rate and fractionation influence the biological processes that govern radiation response, also known as the 4 R's of radiobiology (i.e. repopulation, reoxygenation, redistribution, repair) which occur at different rates [1]. As well, radiation dose is known to impact the degree of radiation-induced vascular damage [204–207] and extent of immune activation [208–210]. Together, these factors are expected to affect the underlying mechanisms and the overall effectiveness of AuNP-based radiosensitization; however, these have not been well studied. In addition, IR has been demonstrated to affect the transport of nanoparticles [211–213]. Using radiation to modulate the tumor microenvironment, and ultimately enhance the accumulation and intra-tumoural distribution of nanoparticles holds great promise in improving the efficacy of AuNP radiosensitizers. Radiation-induced changes in the tumor microenvironment that influence nanoparticle transport are discussed in further detail in a review by Stapleton et al. published in this issue of ADDR. Taken together, careful consideration of the particle parameters and RT treatment scheme must be made in order to obtain biocompatible AuNPs suitable for clinical implementation. To achieve this goal, future research should aim at gaining further understanding of the impact of various parameters (e.g. particle properties, radiations source and energy, fractionation scheme) on the mechanism of radiosensitization. As well, systematic studies evaluating the factors that govern the *in vivo*

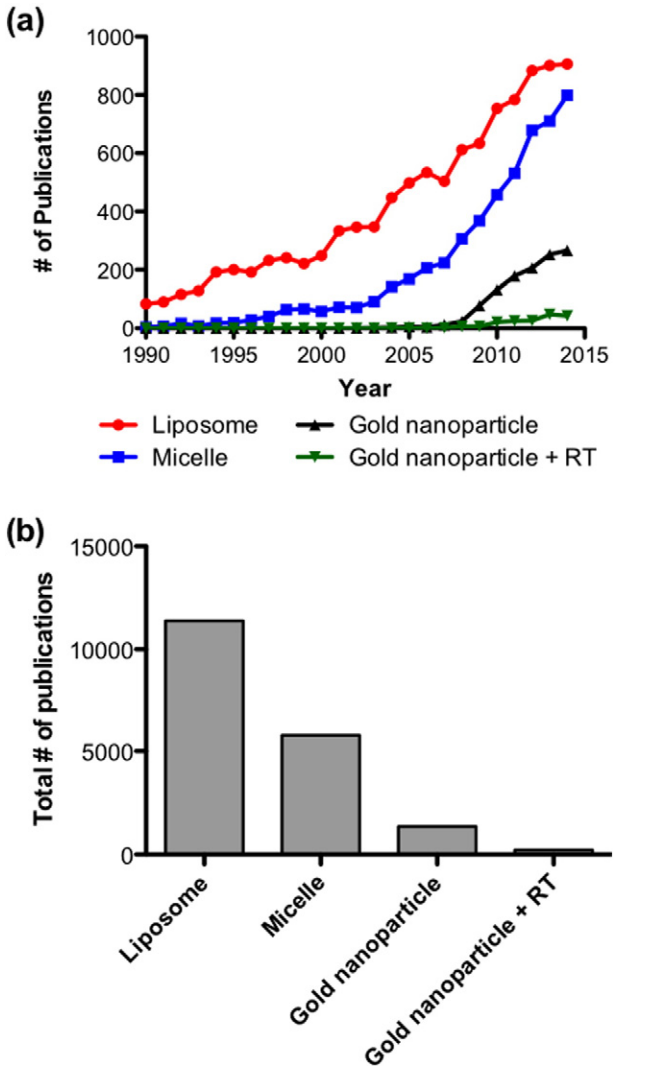

Fig. 5. Number of publications on AuNP radiosensitization compared to other nanoplatforms for drug delivery. Despite the rapid growth in research interest, AuNPs for radiotherapy applications are still in the early stages of development. Data show the number of publications per year (a) and the total number of publications compiled up to September 2015 (b) using Scopus® with search terms "micelle," "liposome" or "gold nanoparticles" each paired with "drug delivery," or "gold nanoparticles" with "radiotherapy."

performance, in particular the *in vivo* fate of AuNPs, are necessary to further guide the design and development of the next generation AuNPs.

5. Conclusions

Over the past decade, the field of AuNP-based radiosensitization has undergone a tremendous growth as demonstrated by the exponential increase in the number of publications on this topic (Fig. 5). Intensive pre-clinical research has enriched our understanding of AuNP radiosensitization beyond what was initially regarded as solely a physical dose enhancement effect. Several mechanisms involving the biological and chemical pathways have been proposed, and the barriers towards successful clinical translation have been identified. Based on the findings to date, recent advancements have focused on exploiting the synthetic versatility of AuNPs to develop multi-functional nanoplatforms, and on expanding the clinical utility of AuNP radiosensitizers. While significant progress has been made, there remain challenges to be overcome, namely the safety concerns and *in vivo* efficacy. In order to address these issues, the precise mechanisms of radiosensitization, especially at the clinically relevant radiation energies, need to be elucidated. As well, the impact of particle- and radiation-related parameters on radiosensitization, and the *in vivo* fate of AuNPs needs to be investigated.

These findings will help guide the design and development of AuNP radiosensitizers with ideal features for clinical implementation. Although clinical translation seems far from reality, we must remember that this field is still in its infancy compared to other well-established nanoplatforms (e.g. block copolymer micelles, liposomes) (Fig. 5). There remain many opportunities to be explored, and areas to be improved. Continued interdisciplinary research efforts are needed to accelerate the translation of AuNP radiosensitizers to clinical practice.

Acknowledgments

C. Allen acknowledges research support from NSERC and GlaxoSmithKline Inc. for the endowed Chair in Pharmaceutics and Drug Delivery. D. Jaffray acknowledges the support through the Mary and Orey Fidani Family Chair in Radiation Physics and the Princess Margaret Cancer Foundation.

References

[1] H. Arnold, Basic Clinical Radiobiology, 4 ed., 2009 London, UK.
[2] G. Delaney, S. Jacob, C. Featherstone, M. Barton, The role of radiotherapy in cancer treatment: estimating optimal utilization from a review of evidence-based clinical guidelines, Cancer 104 (2005) 1129–1137.
[3] D.A. Jaffray, Image-guided radiotherapy: from current concept to future perspectives, Nat. Rev. Clin. Oncol. 9 (2012) 688–699.
[4] L.A. Dawson, D.A. Jaffray, Advances in image-guided radiation therapy, J. Clin. Oncol. 25 (2007) 938–946.
[5] D. Verellen, M. De Ridder, N. Linthout, K. Tournel, G. Soete, G. Storme, Innovations in image-guided radiotherapy, Nat. Rev. Cancer 7 (2007) 949–960.
[6] Intensity Modulated Radiation Therapy Collaborative Working Group, Intensity-modulated radiotherapy: current status and issues of interest, Int. J. Radiat. Oncol. Biol. Phys. 51 (2001) 880–914.
[7] J. Thariat, J.M. Hannoun-Levi, A. Sun Myint, T. Vuong, J.P. Gerard, Past, present, and future of radiotherapy for the benefit of patients, Nat. Rev. Clin. Oncol. 10 (2013) 52–60.
[8] Z.S. Morris, P.M. Harari, Interaction of radiation therapy with molecular targeted agents, J. Clin. Oncol. 32 (2014) 2886–2893.
[9] A.C. Begg, F.A. Stewart, C. Vens, Strategies to improve radiotherapy with targeted drugs, Nat. Rev. Cancer 11 (2011) 239–253.
[10] J. Ye, P. Van Dorpe, W. Van Roy, G. Borghs, G. Maes, Fabrication, characterization, and optical properties of gold nanobowl submonolayer structures, Langmuir 25 (2009) 1822–1827.
[11] C.J. Murphy, L.B. Thompson, D.J. Chernak, J.A. Yang, S.T. Sivapalan, S.P. Boulos, J.Y. Huang, A.M. Alkilany, P.N. Sisco, Gold nanorod crystal growth: from seed-mediated synthesis to nanoscale sculpting, Curr. Opin. Colloid Interface Sci. 16 (2011) 128–134.
[12] C.C. Li, K.L. Shuford, M.H. Chen, E.J. Lee, S.O. Cho, A facile polyol route to uniform gold octahedra with tailorable size and their optical properties, ACS Nano 2 (2008) 1760–1769.
[13] M.Z. Liu, P. Guyot-Sionnest, Mechanism of silver(I)-assisted growth of gold nanorods and bipyramids, J. Phys. Chem. B 109 (2005) 22192–22200.
[14] N.G. Khlebtsov, L.A. Dykman, Optical properties and biomedical applications of plasmonic nanoparticles, J. Quant. Spectrosc. Radiat. Transf. 111 (2010) 1–35.
[15] C.L. Nehl, H.W. Liao, J.H. Hafner, Optical properties of star-shaped gold nanoparticles, Nano Lett. 6 (2006) 683–688.
[16] P. Zhao, N. Li, D. Astruc, State of the art in gold nanoparticle synthesis, Coord. Chem. Rev. 257 (2013) 638–665.
[17] J. Perez-Juste, I. Pastoriza-Santos, L.M. Liz-Marzan, P. Mulvaney, Gold nanorods: synthesis, characterization and applications, Coord. Chem. Rev. 249 (2005) 1870–1901.
[18] S.E. Lohse, C.J. Murphy, The quest for shape control: a history of gold nanorod synthesis, Chem. Mater. 25 (2013) 1250–1261.
[19] M. Grzelczak, J. Perez-Juste, P. Mulvaney, L.M. Liz-Marzan, Shape control in gold nanoparticle synthesis, Chem. Soc. Rev. 37 (2008) 1783–1791.
[20] M.L. Personick, C.A. Mirkin, Making sense of the mayhem behind shape control in the synthesis of gold nanoparticles, J. Am. Chem. Soc. 135 (2013) 18238–18247.
[21] Y.C. Yeh, B. Creran, V.M. Rotello, Gold nanoparticles: preparation, properties, and applications in bionanotechnology, Nanoscale 4 (2012) 1871–1880.
[22] A.M. Alkilany, L.B. Thompson, S.P. Boulos, P.N. Sisco, C.J. Murphy, Gold nanorods: their potential for photothermal therapeutics and drug delivery, tempered by the complexity of their biological interactions, Adv. Drug Deliv. Rev. 64 (2012) 190–199.
[23] K. Kobayashi, J.J. Wei, R. Iida, K. Ijiro, K. Niikura, Surface engineering of nanoparticles for therapeutic applications, Polym. J. 46 (2014) 460–468.
[24] A. Kumari, S.K. Yadav, Cellular interactions of therapeutically delivered nanoparticles, Expert. Opin. Drug Deliv. 8 (2011) 141–151.
[25] A.J. Mieszawska, W.J.M. Mulder, Z.A. Fayad, D.P. Cormode, Multifunctional gold nanoparticles for diagnosis and therapy of disease, Mol. Pharm. 10 (2013) 831–847.
[26] S. Rana, A. Bajaj, R. Mout, V.M. Rotello, Monolayer coated gold nanoparticles for delivery applications, Adv. Drug Deliv. Rev. 64 (2012) 200–216.
[27] P. Ghosh, G. Han, M. De, C.K. Kim, V.M. Rotello, Gold nanoparticles in delivery applications, Adv. Drug Deliv. Rev. 60 (2008) 1307–1315.
[28] R.A. Sperling, P. Rivera Gil, F. Zhang, M. Zanella, W.J. Parak, Biological applications of gold nanoparticles, Chem. Soc. Rev. 37 (2008) 1896–1908.
[29] R. Arvizo, R. Bhattacharya, P. Mukherjee, Gold nanoparticles: opportunities and challenges in nanomedicine, Expert. Opin. Drug Deliv. 7 (2010) 753–763.
[30] K. Saha, S.S. Agasti, C. Kim, X. Li, V.M. Rotello, Gold nanoparticles in chemical and biological sensing, Chem. Rev. 112 (2012) 2739–2779.
[31] C. Kim, E.C. Cho, J.Y. Chen, K.H. Song, L. Au, C. Favazza, Q.A. Zhang, C.M. Cobley, F. Gao, Y.N. Xia, L.H.V. Wang, *In vivo* molecular photoacoustic tomography of melanomas targeted by bioconjugated gold nanocages, ACS Nano 4 (2010) 4559–4564.
[32] P. Huang, L. Bao, C.L. Zhang, J. Lin, T. Luo, D.P. Yang, M. He, Z.M. Li, G. Gao, B. Gao, S. Fu, D.X. Cui, Folic acid-conjugated silica-modified gold nanorods for X-ray/Ct imaging-guided dual-mode radiation and photo-thermal therapy, Biomaterials 32 (2011) 9796–9809.
[33] J.F. Hainfeld, D.N. Slatkin, H.M. Smilowitz, The use of gold nanoparticles to enhance radiotherapy in mice, Phys. Med. Biol. 49 (2004) N309–N315.
[34] K.T. Butterworth, J.A. Coulter, S. Jain, J. Forker, S.J. McMahon, G. Schettino, K.M. Prise, F.J. Currell, D.G. Hirst, Evaluation of cytotoxicity and radiation enhancement using 1.9 Nm gold particles: potential application for cancer therapy, Nanotechnology 21 (2010).
[35] M.Y. Chang, A.L. Shiau, Y.H. Chen, C.J. Chang, H.H. Chen, C.L. Wu, Increased apoptotic potential and dose-enhancing effect of gold nanoparticles in combination with single-dose clinical electron beams on tumor-bearing mice, Cancer Sci. 99 (2008) 1479–1484.
[36] N. Chattopadhyay, Z. Cai, Y.L. Kwon, E. Lechtman, J.P. Pignol, R.M. Reilly, Molecularly targeted gold nanoparticles enhance the radiation response of breast cancer cells and tumor xenografts to X-radiation, Breast Cancer Res. Treat. 137 (2013) 81–91.
[37] N. Chen, W.T. Yang, Y. Bao, H.L. Xu, S.B. Qin, Y. Tu, Bsa capped Au nanoparticle as an efficient sensitizer for glioblastoma tumor radiation therapy, RSC Adv. 5 (2015) 40514–40520.
[38] D.B. Chithrani, S. Jelveh, F. Jalali, M. van Prooijen, C. Allen, R.G. Bristow, R.P. Hill, D.A. Jaffray, Gold nanoparticles as radiation sensitizers in cancer therapy, Radiat. Res. 173 (2010) 719–728.
[39] J.A. Coulter, S. Jain, K.T. Butterworth, L.E. Taggart, G.R. Dickson, S.J. McMahon, W.B. Hyland, M.F. Muir, C. Trainor, A.R. Hounsell, J.M. O'Sullivan, G. Schettino, F.J. Currell, D.G. Hirst, K.M. Prise, Cell type-dependent uptake, localization, and cytotoxicity of 1.9 Nm gold nanoparticles, Int. J. Nanomedicine 7 (2012) 2673–2685.
[40] L. Cui, K. Tse, P. Zahedi, S.M. Harding, G. Zafarana, D.A. Jaffray, R.G. Bristow, C. Allen, Hypoxia and cellular localization influence the radiosensitizing effect of gold nanoparticles (aunps) in breast cancer cells, Radiat. Res. 182 (2014) 475–488.
[41] F. Geng, K. Song, J.Z. Xing, C. Yuan, S. Yan, Q. Yang, J. Chen, B. Kong, Thio-glucose bound gold nanoparticles enhance radio-cytotoxic targeting of ovarian cancer, Nanotechnology 22 (2011) 285101.
[42] S. Jain, J.A. Coulter, K.T. Butterworth, A.R. Hounsell, S.J. McMahon, W.B. Hyland, M.F. Muir, G.R. Dickson, K.M. Prise, F.J. Currell, D.G. Hirst, J.M. O'Sullivan, Gold nanoparticle cellular uptake, toxicity and radiosensitisation in hypoxic conditions, Radiother. Oncol. 110 (2014) 342–347.
[43] S. Jain, J.A. Coulter, A.R. Hounsell, K.T. Butterworth, S.J. McMahon, W.B. Hyland, M.F. Muir, G.R. Dickson, K.M. Prise, F.J. Currell, J.M. O'Sullivan, D.G. Hirst, Cell-specific radiosensitization by gold nanoparticles at megavoltage radiation energies, Int. J. Radiat. Oncol. Biol. Phys. 79 (2011) 531–539.
[44] D.Y. Joh, L. Sun, M. Stangl, A. Al Zaki, S. Murty, P.P. Santoiemma, J.J. Davis, B.C. Baumann, M. Alonso-Basanta, D. Bhang, G.D. Kao, A. Tsourkas, J.F. Dorsey, Selective

targeting of brain tumors with gold nanoparticle-induced radiosensitization, PLoS One 8 (2013).
[45] H. Kaur, G. Pujari, M.K. Semwal, A. Sarma, D.K. Avasthi, *In vitro* studies on radiosensitization effect of glucose capped gold nanoparticles in photon and ion irradiation of Hela cells, Nucl. Instrum. Methods Phys. Res., Sect. B 301 (2013) 7–11.
[46] K. Khoshgard, B. Hashemi, A. Arbabi, M.J. Rasaee, M. Soleimani, Radiosensitization effect of folate-conjugated gold nanoparticles on HeLa cancer cells under orthovoltage superficial radiotherapy techniques, Phys. Med. Biol. 59 (2014) 2249–2263.
[47] T. Kong, J. Zeng, X.P. Wang, X.Y. Yang, J. Yang, S. McQuarrie, A. McEwan, W. Roa, J. Chen, J.Z. Xing, Enhancement of radiation cytotoxicity in breast-cancer cells by localized attachment of gold nanoparticles, Small 4 (2008) 1537–1543.
[48] C.J. Liu, C.H. Wang, S.T. Chen, H.H. Chen, W.H. Leng, C.C. Chien, C.L. Wang, I.M. Kempson, Y. Hwu, T.C. Lai, M. Hsiao, C.S. Yang, Y.J. Chen, G. Margaritondo, Enhancement of cell radiation sensitivity by PEGylated gold nanoparticles, Phys. Med. Biol. 55 (2010) 931–945.
[49] C.J. Liu, C.H. Wang, C.C. Chien, T.Y. Yang, S.T. Chen, W.H. Leng, C.F. Lee, K.H. Lee, Y. Hwu, Y.C. Lee, C.L. Cheng, C.S. Yang, Y.J. Chen, J.H. Je, G. Margaritondo, Enhanced X-ray irradiation-induced cancer cell damage by gold nanoparticles treated by a new synthesis method of polyethylene glycol modification, Nanotechnology 19 (2008) 295104.
[50] Y. Liu, X. Liu, X. Jin, P. He, X. Zheng, Z. Dai, F. Ye, T. Zhao, W. Chen, Q. Li, The dependence of radiation enhancement effect on the concentration of gold nanoparticles exposed to low- and high-LET radiations, Phys. Med. 31 (2015) 210–218.
[51] W.N. Rahman, N. Bishara, T. Ackerly, C.F. He, P. Jackson, C. Wong, R. Davidson, M. Geso, Enhancement of radiation effects by gold nanoparticles for superficial radiation therapy, Nanomed. Nanotechnol. Biol. Med. 5 (2009) 136–142.
[52] W. Roa, X. Zhang, L. Guo, A. Shaw, X. Hu, Y. Xiong, S. Gulavita, S. Patel, X. Sun, J. Chen, R. Moore, J.Z. Xing, Gold nanoparticle sensitize radiotherapy of prostate cancer cells by regulation of the cell cycle, Nanotechnology 20 (2009) 375101.
[53] L.E. Taggart, S.J. McMahon, F.J. Currell, K.M. Prise, K.T. Butterworth, The role of mitochondrial function in gold nanoparticle mediated radiosensitisation, Cancer Nanotechnol. 5 (2014) 5.
[54] C.H. Wang, X.H. Li, Y. Wang, Z. Liu, L. Fu, L.K. Hu, Enhancement of radiation effect and increase of apoptosis in lung cancer cells by thio-glucose-bound gold nanoparticles at megavoltage radiation energies, J. Nanoparticle Res. 15 (2013).
[55] C.H. Wang, Y.H. Jiang, X.H. Li, L.K. Hu, Thioglucose-bound gold nanoparticles increase the radiosensitivity of a triple-negative breast cancer cell line (MDA-MB-231), Breast Cancer 22 (2015) 413–420.
[56] T. Wolfe, D. Chatterjee, J. Lee, J.D. Grant, S. Bhattarai, R. Tailor, G. Goodrich, P. Nicolucci, S. Krishnan, Targeted gold nanoparticles enhance sensitization of prostate tumors to megavoltage radiation therapy *in vivo*, Nanomedicine 11 (2015) 1277–1283.
[57] X. Zhang, J.Z. Xing, J. Chen, L. Ko, J. Amanie, S. Gulavita, N. Pervez, D. Yee, R. Moore, W. Roa, Enhanced radiation sensitivity in prostate cancer by gold-nanoparticles, Clin. Invest. Med. 31 (2008) E160–E167.
[58] X.D. Zhang, D. Wu, X. Shen, J. Chen, Y.M. Sun, P.X. Liu, X.J. Liang, Size-dependent radiosensitization of PEG-coated gold nanoparticles for cancer radiation therapy, Biomaterials 33 (2012) 6408–6419.
[59] X.D. Zhang, J. Chen, Z. Luo, D. Wu, X. Shen, S.S. Song, Y.M. Sun, P.X. Liu, J. Zhao, S. Huo, S. Fan, F. Fan, X.J. Liang, J. Xie, Enhanced tumor accumulation of Sub-2 nm gold nanoclusters for cancer radiation therapy, Adv. Healthcare Mater. 3 (2014) 133–141.
[60] J.F. Hainfeld, F.A. Dilmanian, Z. Zhong, D.N. Slatkin, J.A. Kalef-Ezra, H.M. Smilowitz, Gold nanoparticles enhance the radiation therapy of a murine squamous cell carcinoma, Phys. Med. Biol. 55 (2010) 3045–3059.
[61] J.F. Hainfeld, H.M. Smilowitz, M.J. O'Connor, F.A. Dilmanian, D.N. Slatkin, Gold nanoparticle imaging and radiotherapy of brain tumors in mice, Nanomedicine 8 (2013) 1601–1609.
[62] The time scale in radibiology, in: J. Boag (Ed.), 12th Failla Memorial Lecture, Academic Press, New York 1975, pp. 9–29.
[63] D.F. Regulla, L.B. Hieber, M. Seidenbusch, Physical and biological interface dose effects in tissue due to X-ray-induced release of secondary radiation from metallic gold surfaces, Radiat. Res. 150 (1998) 92–100.
[64] D.M. Herold, I.J. Das, C.C. Stobbe, R.V. Iyer, J.D. Chapman, Gold microspheres: a selective technique for producing biologically effective dose enhancement, Int. J. Radiat. Biol. 76 (2000) 1357–1364.
[65] J.D. Carter, N.N. Cheng, Y.Q. Qu, G.D. Suarez, T. Guo, Nanoscale energy deposition by X-ray absorbing nanostructures, J. Phys. Chem. B 111 (2007) 11622–11625.
[66] Y. Zheng, D.J. Hunting, P. Ayotte, L. Sanche, Radiosensitization of DNA by gold nanoparticles irradiated with high-energy electrons, Radiat. Res. 169 (2008) 19–27.
[67] Y. Zheng, P. Cloutier, D.J. Hunting, L. Sanche, Radiosensitization by gold nanoparticles: comparison of DNA damage induced by low and high-energy electrons, J. Biomed. Nanotechnol. 4 (2008) 469–473.
[68] X.B. Yao, C.N. Huang, X.P. Chen, Y. Zheng, L. Sanche, Chemical radiosensitivity of DNA induced by gold nanoparticles, J. Biomed. Nanotechnol. 11 (2015) 478–485.
[69] Y. Mikami, A. Dhakshinamoorthy, M. Alvaro, H. Garcia, Catalytic activity of unsupported gold nanoparticles, Catal. Sci. Technol. 3 (2013) 58–69.
[70] P. Ionita, B.C. Gilbert, V. Chechik, Radical mechanism of a place-exchange reaction of Au nanoparticles, Angew. Chem. Int. Ed. Engl. 44 (2005) 3720–3722.
[71] P. Ionita, M. Conte, B.C. Gilbert, V. Chechik, Gold nanoparticle-initiated free radical oxidations and halogen abstractions, Org. Biomol. Chem. 5 (2007) 3504–3509.
[72] Z. Zhang, A. Berg, H. Levanon, R.W. Fessenden, D. Meisel, On the interactions of free radicals with gold nanoparticles, J. Am. Chem. Soc. 125 (2003) 7959–7963.
[73] B. Hvolbaek, T.V.W. Janssens, B.S. Clausen, H. Falsig, C.H. Christensen, J.K. Norskov, Catalytic activity of Au nanoparticles, Nano Today 2 (2007) 14–18.
[74] A. Nel, T. Xia, L. Madler, N. Li, Toxic potential of materials at the nanolevel, Science 311 (2006) 622–627.
[75] S. Ito, N. Miyoshi, W.G. Degraff, K. Nagashima, L.J. Kirschenbaum, P. Riesz, Enhancement of 5-aminolevulinic acid-induced oxidative stress on two cancer cell lines by gold nanoparticles, Free Radic. Res. 43 (2009) 1214–1224.
[76] Y. Pan, A. Leifert, D. Ruau, S. Neuss, J. Bornemann, G. Schmid, W. Brandau, U. Simon, W. Jahnen-Dechent, Gold nanoparticles of diameter 1.4 nm trigger necrosis by oxidative stress and mitochondrial damage, Small 5 (2009) 2067–2076.
[77] R. Wahab, S. Dwivedi, F. Khan, Y.K. Mishra, I.H. Hwang, H.S. Shin, J. Musarrat, A.A. Al-Khedhairy, Statistical analysis of gold nanoparticle-induced oxidative stress and apoptosis in myoblast (C2C12) cells, Colloids Surf. B: Biointerfaces 123 (2014) 664–672.
[78] A. Chompoosor, K. Saha, P.S. Ghosh, D.J. Macarthy, O.R. Miranda, Z.J. Zhu, K.F. Arcaro, V.M. Rotello, The role of surface functionality on acute cytotoxicity, ROS generation and DNA damage by cationic gold nanoparticles, Small 6 (2010) 2246–2249.
[79] Y. Tang, Y.F. Shen, L.B. Huang, G.J. Lv, C.H. Lei, X.Y. Fan, F.X. Lin, Y.X. Zhang, L.H. Wu, Y.J. Yang, *In vitro* cytotoxicity of gold nanorods in A549 cells, Environ. Toxicol. Pharmacol. 39 (2015) 871–878.
[80] D. Mateo, P. Morales, A. Avalos, A.I. Haza, Oxidative stress contributes to gold nanoparticle-induced cytotoxicity in human tumor cells, Toxicol. Mech. Methods 24 (2014) 161–172.
[81] M. Misawa, J. Takahashi, Generation of reactive oxygen species induced by gold nanoparticles under X-ray and UV irradiations, Nanomed. Nanotechnol. Biol. Med. 7 (2011) 604–614.
[82] N.N. Cheng, Z. Starkewolf, R.A. Davidson, A. Sharmah, C. Lee, J. Lien, T. Guo, Chemical enhancement by nanomaterials under X-ray irradiation, J. Am. Chem. Soc. 134 (2012) 1950–1953.
[83] S.H. Cho, Estimation of tumour dose enhancement due to gold nanoparticles during typical radiation treatments: a preliminary monte Carlo study, Phys. Med. Biol. 50 (2005) N163–N173.
[84] M. Douglass, E. Bezak, S. Penfold, Monte Carlo investigation of the increased radiation deposition due to gold nanoparticles using kilovoltage and megavoltage photons in a 3D randomized cell model, Med. Phys. 40 (2013).
[85] S.J. McMahon, W.B. Hyland, M.F. Muir, J.A. Coulter, S. Jain, K.T. Butterworth, G. Schettino, G.R. Dickson, A.R. Hounsell, J.M. O'Sullivan, K.M. Prise, D.G. Hirst, F.J. Currell, Nanodosimetric effects of gold nanoparticles in megavoltage radiation therapy, Radiother. Oncol. 100 (2011) 412–416.
[86] R.I. Berbeco, W. Ngwa, G.M. Makrigiorgos, Localized dose enhancement to tumor blood vessel endothelial cells Via megavoltage X-rays and targeted gold nanoparticles: new potential for external beam radiotherapy, Int. J. Radiat. Oncol. Biol. Phys. 81 (2011) 270–276.
[87] J. Liu, Y. Liang, T. Liu, D.K. Li, X.S. Yang, Anti-EGFR-conjugated hollow gold nanospheres enhance radiocytotoxic targeting of cervical cancer at megavoltage radiation energies, Nanoscale Res. Lett. 10 (2015).
[88] N. Burger, A. Biswas, D. Barzan, A. Kirchner, H. Hosser, M. Hausmann, G. Hildenbrand, C. Herskind, F. Wenz, M.R. Veldwijk, A method for the efficient cellular uptake and retention of small modified gold nanoparticles for the radiosensitization of cells, Nanomed. Nanotechnol. Biol. Med. 10 (2014) 1365–1373.
[89] A. Chatterjee, J.L. Magee, Theoretical investigation of the production of strand breaks in DNA by water radicals, Radiat. Prot. Dosim. 13 (1985) 137–140.
[90] W. Lin, Y.W. Huang, X.D. Zhou, Y. Ma, *In vitro* toxicity of silica nanoparticles in human lung cancer cells, Toxicol. Appl. Pharmacol. 217 (2006) 252–259.
[91] C. Carlson, S.M. Hussain, A.M. Schrand, L.K. Braydich-Stolle, K.L. Hess, R.L. Jones, J.J. Schlager, Unique cellular interaction of silver nanoparticles: size-dependent generation of reactive oxygen species, J. Phys. Chem. B 112 (2008) 13608–13619.
[92] T. Xia, M. Kovochich, J. Brant, M. Hotze, J. Sempf, T. Oberley, C. Sioutas, J.I. Yeh, M.R. Wiesner, A.E. Nel, Comparison of the abilities of ambient and manufactured nanoparticles to induce cellular toxicity according to an oxidative stress paradigm, Nano Lett. 6 (2006) 1794–1807.
[93] R. Liu, Y. Wang, Q. Yuan, D. An, J. Li, X. Gao, The Au clusters induce tumor cell apoptosis Via specifically targeting thioredoxin reductase 1 (TrxR1) and suppressing its activity, Chem. Commun. 50 (2014) 10687–10690.
[94] S. Gromer, J.K. Eubel, B.L. Lee, J. Jacob, Human selenoproteins at a glance, Cell. Mol. Life Sci. 62 (2005) 2414–2437.
[95] E.S.J. Arner, A. Holmgren, Physiological functions of thioredoxin and thioredoxin reductase, Eur. J. Biochem. 267 (2000) 6102–6109.
[96] J.G. Fang, J. Lu, A. Holmgren, Thioredoxin reductase is irreversibly modified by curcumin — a novel molecular mechanism for its anticancer activity, J. Biol. Chem. 280 (2005) 25284–25290.
[97] K.F. Tonissen, G. Di Trapani, Thioredoxin system inhibitors as mediators of apoptosis for cancer therapy, Mol. Nutr. Food Res. 53 (2009) 87–103.
[98] Y. Omata, M. Folan, M. Shaw, R.L. Messer, P.E. Lockwood, D. Hobbs, S. Bouillaguet, H. Sano, J.B. Lewis, J.C. Wataha, Sublethal concentrations of diverse gold compounds inhibit mammalian cytosolic thioredoxin reductase (TrxR1), Toxicol. in Vitro 20 (2006) 882–890.
[99] A. Soderberg, B. Sahaf, A. Rosen, Thioredoxin reductase, a redox-active selenoprotein, is secreted by normal and neoplastic cells: presence in human plasma, Cancer Res. 60 (2000) 2281–2289.
[100] J. Lu, E.H. Chew, A. Holmgren, Targeting thioredoxin reductase is a basis for cancer therapy by arsenic trioxide, Proc. Natl. Acad. Sci. U. S. A. 104 (2007) 12288–12293.
[101] A. Citta, A. Folda, A. Bindoli, P. Pigeon, S. Top, A. Vessieres, M. Salmain, G. Jaouen, M.P. Rigobello, Evidence for targeting thioredoxin reductases with ferrocenyl Quinone methides. A possible molecular basis for the antiproliferative effect of hydroxyferrocifens on cancer cells, J. Med. Chem. 57 (2014) 8849–8859.

[102] M.H. Yoo, X.M. Xu, B.A. Carlson, A.D. Patterson, V.N. Gladyshev, D.L. Hatfield, Targeting thioredoxin reductase 1 reduction in cancer cells inhibits self-sufficient growth and DNA replication, PLoS One 2 (2007), e1112.
[103] T.M. Pawlik, K. Keyomarsi, Role of cell cycle in mediating sensitivity to radiotherapy, Int. J. Radiat. Oncol. Biol. Phys. 59 (2004) 928–942.
[104] M.B. Kastan, J. Bartek, Cell-cycle checkpoints and cancer, Nature 432 (2004) 316–323.
[105] B. Kang, M.A. Mackey, M.A. El-Sayed, Nuclear targeting of gold nanoparticles in cancer cells induces DNA damage, causing cytokinesis arrest and apoptosis, J. Am. Chem. Soc. 132 (2010) 1517–1519.
[106] M.A. Mackey, F. Saira, M.A. Mahmoud, M.A. El-Sayed, Inducing cancer cell death by targeting its nucleus: solid gold nanospheres versus hollow gold nanocages, Bioconjug. Chem. 24 (2013) 897–906.
[107] M.A. Mackey, M.A. El-Sayed, Chemosensitization of cancer cells Via gold nanoparticle-induced cell cycle regulation, Photochem. Photobiol. 90 (2014) 306–312.
[108] W.C. Xu, T. Luo, P. Li, C.Q. Zhou, D.X. Cui, B. Pang, Q.S. Ren, S. Fu, RGD-conjugated gold nanorods induce radiosensitization in melanoma cancer cells by downregulating alpha(V)beta(3) expression, Int. J. Nanomedicine 7 (2012) 915–924.
[109] T. Helleday, E. Petermann, C. Lundin, B. Hodgson, R.A. Sharma, DNA repair pathways as targets for cancer therapy, Nat. Rev. Cancer 8 (2008) 193–204.
[110] J.P. Banath, P.L. Olive, Expression of phosphorylated histone H2AX as a surrogate of cell killing by drugs that create DNA double-strand breaks, Cancer Res. 63 (2003) 4347–4350.
[111] A. Choudhury, A. Cuddihy, R.G. Bristow, Radiation and new molecular agents part I: targeting ATM-ATR checkpoints, DNA repair, and the proteasome, Semin. Radiat. Oncol. 16 (2006) 51–58.
[112] P. Wust, B. Hildebrandt, G. Sreenivasa, B. Rau, J. Gellermann, H. Riess, R. Felix, P.M. Schlag, Hyperthermia in combined treatment of cancer, Lancet Oncol. 3 (2002) 487–497.
[113] B. Hildebrandt, P. Wust, O. Ahlers, A. Dieing, G. Sreenivasa, T. Kerner, R. Felix, H. Riess, The cellular and molecular basis of hyperthermia, Crit. Rev. Oncol. Hematol. 43 (2002) 33–56.
[114] P. Kaur, M.D. Hurwitz, S. Krishnan, A. Asea, Combined hyperthermia and radiotherapy for the treatment of cancer, Cancers (Basel) 3 (2011) 3799–3823.
[115] M.R. Horsman, J. Overgaard, Hyperthermia: a potent enhancer of radiotherapy, Clin. Oncol. 19 (2007) 418–426.
[116] L.R. Hirsch, R.J. Stafford, J.A. Bankson, S.R. Sershen, B. Rivera, R.E. Price, J.D. Hazle, N.J. Halas, J.L. West, Nanoshell-mediated near-infrared thermal therapy of tumors under magnetic resonance guidance, Proc. Natl. Acad. Sci. U. S. A. 100 (2003) 13549–13554.
[117] L.C. Kennedy, L.R. Bickford, N.A. Lewinski, A.J. Coughlin, Y. Hu, E.S. Day, J.L. West, R.A. Drezek, A new era for cancer treatment: gold-nanoparticle-mediated thermal therapies, Small 7 (2011) 169–183.
[118] E.C. Dreaden, M.A. Mackey, X.H. Huang, B. Kang, M.A. El-Sayed, Beating cancer in multiple ways using nanogold, Chem. Soc. Rev. 40 (2011) 3391–3404.
[119] P. Diagaradjane, A. Shetty, J.C. Wang, A.M. Elliott, J. Schwartz, S. Shentu, H.C. Park, A. Deorukhkar, R.J. Stafford, S.H. Cho, J.W. Tunnell, J.D. Hazle, S. Krishnan, Modulation of *in vivo* tumor radiation response Via gold nanoshell-mediated vascular-focused hyperthermia: characterizing an integrated antihypoxic and localized vascular disrupting targeting strategy, Nano Lett. 8 (2008) 1492–1500.
[120] J.F. Hainfeld, L. Lin, D.N. Slatkin, F.A. Dilmanian, T.M. Vadas, H.M. Smilowitz, Gold nanoparticle hyperthermia reduces radiotherapy dose, Nanomed. Nanotechnol. Biol. Med. 10 (2014) 1609–1617.
[121] Y.S. Yang, R.P. Carney, F. Stellacci, D.J. Irvine, Enhancing radiotherapy by lipid nanocapsule-mediated delivery of amphiphilic gold nanoparticles to intracellular membranes, ACS Nano 8 (2014) 8992–9002.
[122] A. Al Zaki, D. Joh, Z.L. Cheng, A.L.B. De Barros, G. Kao, J. Dorsey, A. Tsourkas, Gold-loaded polymeric micelles for computed tomography-guided radiation therapy treatment and radiosensitization, ACS Nano 8 (2014) 104–112.
[123] C. McQuade, A. Al Zaki, Y. Desai, M. Vido, T. Sakhuja, Z.L. Cheng, R.J. Hickey, D. Joh, S.J. Park, G. Kao, J.F. Dorsey, A. Tsourkas, A multifunctional nanoplatform for imaging, radiotherapy, and the prediction of therapeutic response, Small 11 (2015) 834–843.
[124] L. Vigderman, E.R. Zubarev, Therapeutic platforms based on gold nanoparticles and their covalent conjugates with drug molecules, Adv. Drug Deliv. Rev. 65 (2013) 663–676.
[125] R. Cao-Milan, L.M. Liz-Marzan, Gold nanoparticle conjugates: recent advances toward clinical applications, Expert. Opin. Drug Deliv. 11 (2014) 741–752.
[126] T.Y. Seiwert, J.K. Salama, E.E. Vokes, The concurrent chemoradiation paradigm — general principles, Nat. Clin. Pract. Oncol. 4 (2007) 86–100.
[127] G.D. Wilson, S.M. Bentzen, P.M. Harari, Biologic basis for combining drugs with radiation, Semin. Radiat. Oncol. 16 (2006) 2–9.
[128] V. Gregoire, W.N. Hittelman, J.F. Rosier, L. Milas, Chemo-radiotherapy: radiosensitizing nucleoside analogues (review), Oncol. Rep. 6 (1999) 949–957.
[129] S. Girdhani, S.M. Bhosle, S.A. Thulsidas, A. Kumar, K.P. Mishra, Potential of radiosensitizing agents in cancer chemo-radiotherapy, J. Cancer Res. Ther. 1 (2005) 129–131.
[130] A.C. Begg, Cisplatin and radiation: interaction probabilities and therapeutic possibilities, Int. J. Radiat. Oncol. Biol. Phys. 19 (1990) 1183–1189.
[131] L.X. Yang, E.B. Douple, J.A. O'Hara, H.J. Wang, Production of DNA double-strand breaks by interactions between carboplatin and radiation: a potential mechanism for radiopotentiation, Radiat. Res. 143 (1995) 309–315.
[132] E.E. Vokes, R.R. Weichselbaum, Concomitant chemoradiotherapy: rationale and clinical experience in patients with solid tumors, J. Clin. Oncol. 8 (1990) 911–934.
[133] R.C. Richmond, Toxic variability and radiation sensitization by dichlorodiammineplatinum(II) complexes in salmonella typhimurium cells, Radiat. Res. 99 (1984) 596–608.
[134] Y. Zheng, L. Sanche, Gold nanoparticles enhance DNA damage induced by anti-cancer drugs and radiation, Radiat. Res. 172 (2009) 114–119.
[135] S.-M. Lee, D.-H. Tsai, V.A. Hackley, M.W. Brechbiel, R.F. Cook, Surface-engineered nanomaterials as X-ray absorbing adjuvant agents for auger-mediated chemo-radiation, Nanoscale 5 (2013) 5252–5256.
[136] S. Setua, M. Ouberai, S.G. Piccirillo, C. Watts, M. Welland, Cisplatin-tethered gold nanospheres for multimodal chemo-radiotherapy of glioblastoma, Nanoscale 6 (2014) 10865–10873.
[137] J.A. Bonner, T.S. Lawrence, Doxorubicin decreases the repair of radiation-induced DNA damage, Int. J. Radiat. Biol. 57 (1990) 55–64.
[138] H.Y. Zhou, Y. Zhang, G.X. Su, S.M. Zhai, B. Yan, Enhanced cancer cell killing by a targeting gold nanoconstruct with doxorubicin payload under X-ray irradiation, RSC Adv. 3 (2013) 21596–21603.
[139] Z.B. Starkewolf, L. Miyachi, J. Wong, T. Guo, X-ray triggered release of doxorubicin from nanoparticle drug carriers for cancer therapy, Chem. Commun. 49 (2013) 2545–2547.
[140] J. Park, J. Park, E.J. Ju, S.S. Park, J. Choi, J.H. Lee, K.J. Lee, S.H. Shin, E.J. Ko, I. Park, C. Kim, J.J. Hwang, J.S. Lee, S.Y. Song, S.Y. Jeong, E.K. Choi, Multifunctional hollow gold nanoparticles designed for triple combination therapy and Ct imaging, J. Control. Release 207 (2015) 77–85.
[141] A.K. Nowinski, A.D. White, A.J. Keefe, S.Y. Jiang, Biologically inspired stealth peptide-capped gold nanoparticles, Langmuir 30 (2014) 1864–1870.
[142] P. Rathinaraj, K. Lee, Y. Choi, S.-Y. Park, O. Kwon, I.-K. Kang, Targeting and molecular imaging of HepG2 cells using surface-functionalized gold nanoparticles, J. Nanoparticle Res. 17 (2015) 1–12.
[143] P. Rathinaraj, K. Lee, S.Y. Park, I.K. Kang, Targeted images of KB cells using folate-conjugated gold nanoparticles, Nanoscale Res. Lett. 10 (2015) 5.
[144] Z.W. Zhang, J. Jia, Y.Q. Lai, Y.Y. Ma, J. Weng, L.P. Sun, Conjugating folic acid to gold nanoparticles through glutathione for targeting and detecting cancer cells, Bioorg. Med. Chem. 18 (2010) 5528–5534.
[145] J.F. Hainfeld, M.J. O'Connor, F.A. Dilmanian, D.N. Slatkin, D.J. Adams, H.M. Smilowitz, Micro-Ct enables microlocalisation and quantification of HER2-targeted gold nanoparticles within tumour regions, Br. J. Radiol. 84 (2011) 526–533.
[146] H.W. Kao, Y.Y. Lin, C.C. Chen, K.H. Chi, D.C. Tien, C.C. Hsia, W.J. Lin, F.D. Chen, M.H. Lin, H.E. Wang, Biological characterization of cetuximab-conjugated gold nanoparticles in a tumor animal model, Nanotechnology 25 (2014).
[147] S. Bhattacharyya, M. Gonzalez, J.D. Robertson, R. Bhattacharya, P. Mukherjee, A simple synthesis of a targeted drug delivery system with enhanced cytotoxicity, Chem. Commun. 47 (2011) 8530–8532.
[148] N. Chattopadhyay, Z.L. Cai, J.P. Pignol, B. Keller, E. Lechtman, R. Bendayan, R.M. Reilly, Design and characterization of HER-2-targeted gold nanoparticles for enhanced X-radiation treatment of locally advanced breast cancer, Mol. Pharm. 7 (2010) 2194–2206.
[149] W. Roa, Y.P. Xiong, J. Chen, X.Y. Yang, K. Song, X.H. Yang, B.H. Kong, J. Wilson, J.Z. Xing, Pharmacokinetic and toxicological evaluation of multi-functional thiol-6-fluoro-6-deoxy-D-glucose gold nanoparticles *in vivo*, Nanotechnology 23 (2012).
[150] F. Geng, J.Z. Xing, J. Chen, R. Yang, Y. Hao, K. Song, B.H. Kong, PEGylated glucose gold nanoparticles for improved in-vivo Bio-distribution and enhanced radiotherapy on cervical cancer, J. Biomed. Nanotechnol. 10 (2014) 1205–1216.
[151] P. Vaupel, A. Mayer, Hypoxia in cancer: significance and impact on clinical outcome, Cancer Metastasis Rev. 26 (2007) 225–239.
[152] J.M. Brown, Tumor hypoxia in cancer therapy, Methods Enzymol. 435 (2007) 297–321.
[153] S. Rockwell, I.T. Dobrucki, E.Y. Kim, S.T. Marrison, V.T. Vu, Hypoxia and radiation therapy: past history, ongoing research, and future promise, Curr. Mol. Med. 9 (2009) 442–458.
[154] P. Vaupel, Tumor microenvironmental physiology and its implications for radiation oncology, Semin. Radiat. Oncol. 14 (2004) 198–206.
[155] L.H. Gray, A.D. Conger, M. Ebert, S. Hornsey, O.C.A. Scott, The concentration of oxygen dissolved in tissues at the time of irradiation as a factor in radiotherapy, Br. J. Radiol. 26 (1953) 638–648.
[156] D. Schulz-Ertner, H. Tsujii, Particle radiation therapy using proton and heavier ion beams, J. Clin. Oncol. 25 (2007) 953–964.
[157] G.E. Laramore, Role of particle radiotherapy in the management of head and neck cancer, Curr. Opin. Oncol. 21 (2009) 224–231.
[158] A.M. Allen, T. Pawlicki, L. Dong, E. Fourkal, M. Buyyounouski, K. Cengel, J. Plastaras, M.K. Bucci, T.I. Yock, L. Bonilla, R. Price, E.E. Harris, A.A. Konski, An evidence based review of proton beam therapy: the report of ASTRO's emerging technology committee, Radiother. Oncol. 103 (2012) 8–11.
[159] Proton therapy around the world, http://www.proton-cancer-treatment.com/proton-therapy/proton-therapy-around-the-world August 31, 2015.
[160] J.K. Kim, S.J. Seo, K.H. Kim, T.J. Kim, M.H. Chung, K.R. Kim, T.K. Yang, Therapeutic application of metallic nanoparticles combined with particle-induced X-ray emission effect, Nanotechnology 21 (2010) 425102.
[161] J.K. Kim, S.J. Seo, H.T. Kim, K.H. Kim, M.H. Chung, K.R. Kim, S.J. Ye, Enhanced proton treatment in mouse tumors through proton irradiated nanoradiator effects on metallic nanoparticles, Phys. Med. Biol. 57 (2012) 8309–8323.
[162] J.C. Polf, L.F. Bronk, W.H. Driessen, W. Arap, R. Pasqualini, M. Gillin, Enhanced relative biological effectiveness of proton radiotherapy in tumor cells with internalized gold nanoparticles, Appl. Phys. Lett. 98 (2011) 193702.
[163] Y. Lin, S.J. McMahon, M. Scarpelli, H. Paganetti, J. Schuemann, Comparing gold Nanoparticle enhanced radiotherapy with protons, megavoltage photons and kilovoltage photons: a monte Carlo simulation, Phys. Med. Biol. 59 (2014) 7675–7689.
[164] Y.T. Lin, S.J. McMahon, H. Paganetti, J. Schuemann, Biological modeling of gold nanoparticle enhanced radiotherapy for proton therapy, Phys. Med. Biol. 60 (2015) 4149–4168.

[165] R. Hirayama, A. Ito, M. Tomita, T. Tsukada, F. Yatagai, M. Noguchi, Y. Matsumoto, Y. Kase, K. Ando, R. Okayasu, Y. Furusawa, Contributions of direct and indirect actions in cell killing by high-LET radiations, Radiat. Res. 171 (2009) 212–218.
[166] S.K. Libutti, G.F. Paciotti, A.A. Byrnes, H.R. Alexander, W.E. Gannon, M. Walker, G.D. Seidel, N. Yuldasheva, L. Tamarkin, Phase I and pharmacokinetic studies of Cyt-6091, a novel PEGylated colloidal gold-RhTNF nanomedicine, Clin. Cancer Res. 16 (2010) 6139–6149.
[167] Z. Lin, N.A. Monteiro-Riviere, J.E. Riviere, Pharmacokinetics of metallic nanoparticles, Wiley Interdiscip. Rev. Nanomed. Nanobiotechnol. 7 (2015) 189–217.
[168] N. Khlebtsov, L. Dykman, Biodistribution and toxicity of engineered gold nanoparticles: a review of in vitro and *in vivo* studies, Chem. Soc. Rev. 40 (2011) 1647–1671.
[169] E.C. Dreaden, L.A. Austin, M.A. Mackey, M.A. El-Sayed, Size matters: gold nanoparticles in targeted cancer drug delivery, Ther. Deliv. 3 (2012) 457–478.
[170] N.P. Truong, M.R. Whittaker, C.W. Mak, T.P. Davis, The importance of nanoparticle shape in cancer drug delivery, Expert. Opin. Drug Deliv. 12 (2015) 129–142.
[171] B. Derjaguin, L. Landau, Theory of the stability of strongly charged lyophobic sols and of the adhesion of strongly charged-particles in solutions of electrolytes, Prog. Surf. Sci. 43 (1993) 30–59.
[172] G. Wang, W. Sun, Optical limiting of gold nanoparticle aggregates induced by electrolytes, J. Phys. Chem. B 110 (2006) 20901–20905.
[173] R. Pamies, J. Cifre, V. Espín, M. Collado-González, F. Baños, J. de la Torre, Aggregation behaviour of gold nanoparticles in saline aqueous media, J. Nanoparticle Res. 16 (2014) 1–11.
[174] A. Albanese, W.C.W. Chan, Effect of gold nanoparticle aggregation on cell uptake and toxicity, ACS Nano 5 (2011) 5478–5489.
[175] J. Lazarovits, Y.Y. Chen, E.A. Sykes, W.C.W. Chan, Nanoparticle-blood interactions: the implications on solid tumour targeting, Chem. Commun. 51 (2015) 2756–2767.
[176] M. Hayat, Colloidal gold, Principles, Methods and Applications, Academic Press, San Diego, 1989.
[177] E.D. Kaufman, J. Belyea, M.C. Johnson, Z.M. Nicholson, J.L. Ricks, P.K. Shah, M. Bayless, T. Pettersson, Z. Feldoto, E. Blomberg, P. Claesson, S. Franzen, Probing protein adsorption onto mercaptoundecanoic acid stabilized gold nanoparticles and surfaces by quartz crystal microbalance and zeta-potential measurements, Langmuir 23 (2007) 6053–6062.
[178] A. Albanese, C.D. Walkey, J.B. Olsen, H.B. Guo, A. Emili, W.C.W. Chan, Secreted biomolecules alter the biological identity and cellular interactions of nanoparticles, ACS Nano 8 (2014) 5515–5526.
[179] K.Y. Huang, H.L. Ma, J. Liu, S.D. Huo, A. Kumar, T. Wei, X. Zhang, S.B. Jin, Y.L. Gan, P.C. Wang, S.T. He, X.N. Zhang, X.J. Liang, Size-dependent localization and penetration of ultrasmall gold nanoparticles in cancer cells, multicellular spheroids, and tumors *in vivo*, ACS Nano 6 (2012) 4483–4493.
[180] S.D. Huo, H.L. Ma, K.Y. Huang, J. Liu, T. Wei, S.B. Jin, J.C. Zhang, S.T. He, X.J. Liang, Superior penetration and retention behavior of 50 nm gold nanoparticles in tumors, Cancer Res. 73 (2013) 319–330.
[181] B.D. Chithrani, A.A. Ghazani, W.C.W. Chan, Determining the size and shape dependence of gold nanoparticle uptake into mammalian cells, Nano Lett. 6 (2006) 662–668.
[182] B.D. Chithrani, W.C.W. Chan, Elucidating the mechanism of cellular uptake and removal of protein-coated gold nanoparticles of different sizes and shapes, Nano Lett. 7 (2007) 1542–1550.
[183] F.X. Xiao, Y. Zheng, P. Cloutier, Y.H. He, D. Hunting, L. Sanche, On the role of low-energy electrons in the radiosensitization of DNA by gold nanoparticles, Nanotechnology 22 (2011).
[184] S.J. McMahon, W.B. Hyland, M.F. Muir, J.A. Coulter, S. Jain, K.T. Butterworth, G. Schettino, G.R. Dickson, A.R. Hounsell, J.M. O'Sullivan, K.M. Prise, D.G. Hirst, F.J. Currell, Biological consequences of nanoscale energy deposition near irradiated heavy atom nanoparticles, Sci. Rep. 1 (2011) 18.
[185] C.C. Berry, J.M. de la Fuente, M. Mullin, S.W.L. Chu, A.S.G. Curtis, Nuclear localization of Hiv-1 Tat functionalized gold nanoparticles, IEEE Trans. Nanobiosci. 6 (2007) 262–269.
[186] P. Nativo, I.A. Prior, M. Brust, Uptake and intracellular fate of surface-modified gold nanoparticles, ACS Nano 2 (2008) 1639–1644.
[187] A.G. Tkachenko, H. Xie, Y.L. Liu, D. Coleman, J. Ryan, W.R. Glomm, M.K. Shipton, S. Franzen, D.L. Feldheim, Cellular trajectories of peptide-modified gold particle complexes: comparison of nuclear localization signals and peptide transduction domains, Bioconjug. Chem. 15 (2004) 482–490.
[188] A.G. Tkachenko, H. Xie, D. Coleman, W. Glomm, J. Ryan, M.F. Anderson, S. Franzen, D.L. Feldheim, Multifunctional gold nanoparticle-peptide complexes for nuclear targeting, J. Am. Chem. Soc. 125 (2003) 4700–4701.
[189] J.M. de la Fuente, C.C. Berry, Tat peptide as an efficient molecule to translocate gold nanoparticles into the cell nucleus, Bioconjug. Chem. 16 (2005) 1176–1180.
[190] C. Yang, J. Uertz, D. Yohan, B.D. Chithrani, Peptide modified gold nanoparticles for improved cellular uptake, nuclear transport, and intracellular retention, Nanoscale 6 (2014) 12026–12033.
[191] D. Mandal, A. Maran, M.J. Yaszemski, M.E. Bolander, G. Sarkar, Cellular uptake of gold nanoparticles directly cross-linked with carrier peptides by osteosarcoma cells, J. Mater. Sci. Mater. Med. 20 (2009) 347–350.
[192] E. Oh, J.B. Delehanty, K.E. Sapsford, K. Susumu, R. Goswami, J.B. Blanco-Canosa, P.E. Dawson, J. Granek, M. Shoff, Q. Zhang, P.L. Goering, A. Huston, I.L. Medintz, Cellular uptake and fate of PEGylated gold nanoparticles is dependent on both cell-penetration peptides and particle size, ACS Nano 5 (2011) 6434–6448.
[193] Z. Krpetic, S. Saleemi, I.A. Prior, V. See, R. Qureshi, M. Brust, Negotiation of intracellular membrane barriers by Tat-modified gold nanoparticles, ACS Nano 5 (2011) 5195–5201.
[194] D.B. Chithrani, Intracellular uptake, transport, and processing of gold nanostructures, Mol. Membr. Biol. 27 (2010) 299–311.
[195] Y. Pan, S. Neuss, A. Leifert, M. Fischler, F. Wen, U. Simon, G. Schmid, W. Brandau, W. Jahnen-Dechent, Size-dependent cytotoxicity of gold nanoparticles, Small 3 (2007) 1941–1949.
[196] S. Fraga, A. Brandao, M.E. Soares, T. Morais, J.A. Duarte, L. Pereira, L. Soares, C. Neves, E. Pereira, L. Bastos Mde, H. Carmo, Short- and long-term distribution and toxicity of gold nanoparticles in the rat after a single-dose intravenous administration, Nanomedicine 10 (2014) 1757–1766.
[197] E. Sadauskas, G. Danscher, M. Stoltenberg, U. Vogel, A. Larsen, H. Wallin, Protracted elimination of gold nanoparticles from mouse liver, Nanomedicine 5 (2009) 162–169.
[198] M.A.K. Abdelhalim, B.M. Jarrar, Histological alterations in the liver of rats induced by different gold nanoparticle sizes, doses and exposure duration, J. Nanobiotechnol. 10 (2012).
[199] M.A.K. Abdelhalim, B.M. Jarrar, Gold nanoparticles induced cloudy swelling to hydropic degeneration, cytoplasmic hyaline vacuolation, polymorphism, binucleation, karyopyknosis, karyolysis, karyorrhexis and necrosis in the liver, Lipids Health Dis. 10 (2011).
[200] S.K. Balasubramanian, J. Jittiwat, J. Manikandan, C.N. Ong, L.E. Yu, W.Y. Ong, Biodistribution of gold nanoparticles and gene expression changes in the liver and spleen after intravenous administration in rats, Biomaterials 31 (2010) 2034–2042.
[201] W.S. Cho, M. Cho, J. Jeong, M. Choi, H.Y. Cho, B.S. Han, S.H. Kim, H.O. Kim, Y.T. Lim, B.H. Chung, J. Jeong, Acute toxicity and pharmacokinetics of 13 nm-sized PEG-coated gold nanoparticles, Toxicol. Appl. Pharmacol. 236 (2009) 16–24.
[202] X.D. Zhang, D. Wu, X. Shen, P.X. Liu, F.Y. Fan, S.J. Fan, *In vivo* renal clearance, biodistribution, toxicity of gold nanoclusters, Biomaterials 33 (2012) 4628–4638.
[203] J.H. Hwang, S.J. Kim, Y.H. Kim, J.R. Noh, G.T. Gang, B.H. Chung, N.W. Song, C.H. Lee, Susceptibility to gold nanoparticle-induced hepatotoxicity is enhanced in a mouse model of nonalcoholic steatohepatitis, Toxicology 294 (2012) 27–35.
[204] G.O. Ahn, J.M. Brown, Matrix metalloproteinase-9 is required for tumor vasculogenesis but not for angiogenesis: role of bone marrow-derived myelomonocytic cells, Cancer Cell 13 (2008) 193–205.
[205] M. Garcia-Barros, F. Paris, C. Cordon-Cardo, D. Lyden, S. Rafii, A. Haimovitz-Friedman, Z. Fuks, R. Kolesnick, Tumor response to radiotherapy regulated by endothelial cell apoptosis, Science 300 (2003) 1155–1159.
[206] H.E. Barker, J.T. Paget, A.A. Khan, K.J. Harrington, The tumour microenvironment after radiotherapy: mechanisms of resistance and recurrence, Nat. Rev. Cancer 15 (2015) 409–425.
[207] Z. Fuks, R. Kolesnick, Engaging the vascular component of the tumor response, Cancer Cell 8 (2005) 89–91.
[208] A.A. Lugade, J.P. Moran, S.A. Gerber, R.C. Rose, J.G. Frelinger, E.M. Lord, Local radiation therapy of B16 melanoma tumors increases the generation of tumor antigen-specific effector cells that traffic to the tumor, J. Immunol. 174 (2005) 7516–7523.
[209] Y.J. Lee, S.L. Auh, Y.G. Wang, B. Burnette, Y. Wang, Y.R. Meng, M. Beckett, R. Sharma, R. Chin, T. Tu, R.R. Weichselbaum, Y.X. Fu, Therapeutic effects of ablative radiation on local tumor require CD8(+) T cells: changing strategies for cancer treatment, Blood 114 (2009) 589–595.
[210] M.Z. Dewan, A.E. Galloway, N. Kawashima, J.K. Dewyngaert, J.S. Babb, S.C. Formenti, S. Demaria, Fractionated but not single-dose radiotherapy induces an immune-mediated abscopal effect when combined with anti-CTLA-4 antibody, Clin. Cancer Res. 15 (2009) 5379–5388.
[211] C.D.L. Davies, L.M. Lundstrom, J. Frengen, L. Eikenes, O.S. Bruland, O. Kaahus, M.H.B. Hjelstuen, C. Brekken, Radiation improves the distribution and uptake of liposomal doxorubicin (Caelyx) in human osteosarcoma xenografts, Cancer Res. 64 (2004) 547–553.
[212] T. Lammers, P. Peschke, R. Kuhnlein, V. Subr, K. Ulbriich, J. Debus, P. Huber, W. Hennink, G. Storm, Effect of radiotherapy and hyperthermia on the tumor accumulation of hpma copolymer-based drug delivery systems, J. Control. Release 117 (2007) 333–341.
[213] D.Y. Joh, G.D. Kao, S. Murty, M. Stangl, L. Sun, A. Al Zaki, X.S. Xu, S.M. Hahn, A. Tsourkas, J.F. Dorsey, Theranostic gold nanoparticles modified for durable systemic circulation effectively and safely enhance the radiation therapy of human sarcoma cells and tumors, Transl. Oncol. 6 (2013) 722–731.